Journal of Gastroenterology and Hepatology

JGHF

doi:10.1111/j.1440-1746.2010.06470.x

MECHANISMS OF GASTROINTESTINAL, PANCREATIC AND LIVER DISEASES

Animal model for study of human hepatitis viruses

Kazuaki Chayama,*,† C Nelson Hayes,*,† Nobuhiko Hiraga,*,† Hiromi Abe,*,† Masataka Tsuge*,† and Michio Imamura*,†

*Department of Medicine and Molecular Science, Division of Frontier Medical Science, Programs for Biomedical Research, Graduate School of Biomedical Sciences, Hiroshima University, and †Liver Research Project Center, Hiroshima, Japan

Key words
hepatitis B virus, hepatitis C virus, uPA/scid mouse model.

Accepted for publication 26 July 2010.

Correspondence
Professor Kazuaki Chayama, Department of Medical and Molecular Science, Division of Frontier Medical Science, Programs for Biomedical Research, Graduate school of Biomedical Science, Hiroshima University, 1-2-3 Kasumi, Minami-ku, Hiroshima 734-8551, Japan. Email: chayama@hiroshima-u.ac.jp

Abstract

Human hepatitis B virus (HBV) and hepatitis C virus (HCV) infect only chimpanzees and humans. Analysis of both viruses has long been hampered by the absence of a small animal model. The recent development of human hepatocyte chimeric mice has enabled us to carry out studies on viral replication and cellular changes induced by replication of human hepatitis viruses. Various therapeutic agents have also been tested using this model. In the present review, we summarize published studies using chimeric mice and discuss the merits and shortcomings of this model.

Introduction

Hepatitis B virus (HBV) and hepatitis C virus (HCV) are pathogens that cause chronic infection in humans. There are 360 million and 170 million people infected worldwide with HBV or HCV, respectively.[1,2] Infected individuals develop acute hepatitis, chronic hepatitis and liver cirrhosis. The viruses are also important causative agents of hepatocellular carcinoma, especially in the Asia–Pacific region.[3] Study of the biology and development of therapies for each virus has long been hampered by the lack of a small animal model that supports hepatitis virus infection. This is probably as a result of the lack of receptor molecules necessary for viral infection in animal liver cells.

Transgenic mice that express over-length HBV-DNA export viral particles into the serum,[4] and such animals can be used to evaluate antiviral agents,[5–7] as well as HBV-targeted siRNA[8]. However, the virus life cycle is not established in this model, and it is inappropriate for studying drug-resistant HBV strains. Accordingly, researchers attempted to transplant human hepatocytes into mice. The development of the trimera mouse was one such attempt, in which human hepatocytes were transplanted under the kidney capsule of immune-deficient mice after lethal irradiation.[9,10] However, the number of hepatocytes that could survive on the kidney capsule was small, and normal liver architecture was not present. Although 85% of HBV-inoculated animals developed HBV viremia, the titer was less than 10^5 virus particles or IU/mL.[9] Similarly, 85% of HCV-inoculated animals also developed viremia,[10] but the level of the viremia only reached 10^5/mL. Thus, the advent of human hepatocyte transplanted uPA/scid mice has provided the first really useful model for acute and chronic infections of human hepatitis virus.

Human liver cell transplanted uPA/scid mice

Transgenic mice in which the urokinase gene is driven by the human albumin promoter/enhancer were developed and shown to have accelerated hepatocyte death and consequent chronic stimulation of hepatocyte growth.[11] Transplanted rat hepatocytes proliferated and repopulated injured livers in immunodeficient uPA mice, which were produced by mating uPA transgenic mice with scid mice.[12] Human hepatocytes were then transplanted into uPA/scid mice; these cells proliferated and replaced the apoptotic mice liver cells (Fig. 1).

Such human hepatocyte chimeric mice have been shown to be susceptible to both HBV[16] and HCV[17] infections. Repopulation levels by human hepatocytes have been estimated by measuring human albumin levels in mouse serum. Replication levels of both HBV[13] and HCV[17] were higher in mice in which the repopulation index was higher. A unique attempt to remove mouse residual liver cells with the herpes simplex virus type-1 thymidine kinase (HSVtk)/ganciclovir (GCV) system failed to result in a higher repopulation rate as a result of damage to the transplanted human hepatocyte caused by bystander effects.[18] Despite this, mice with livers that have been highly repopulated with human hepatocytes

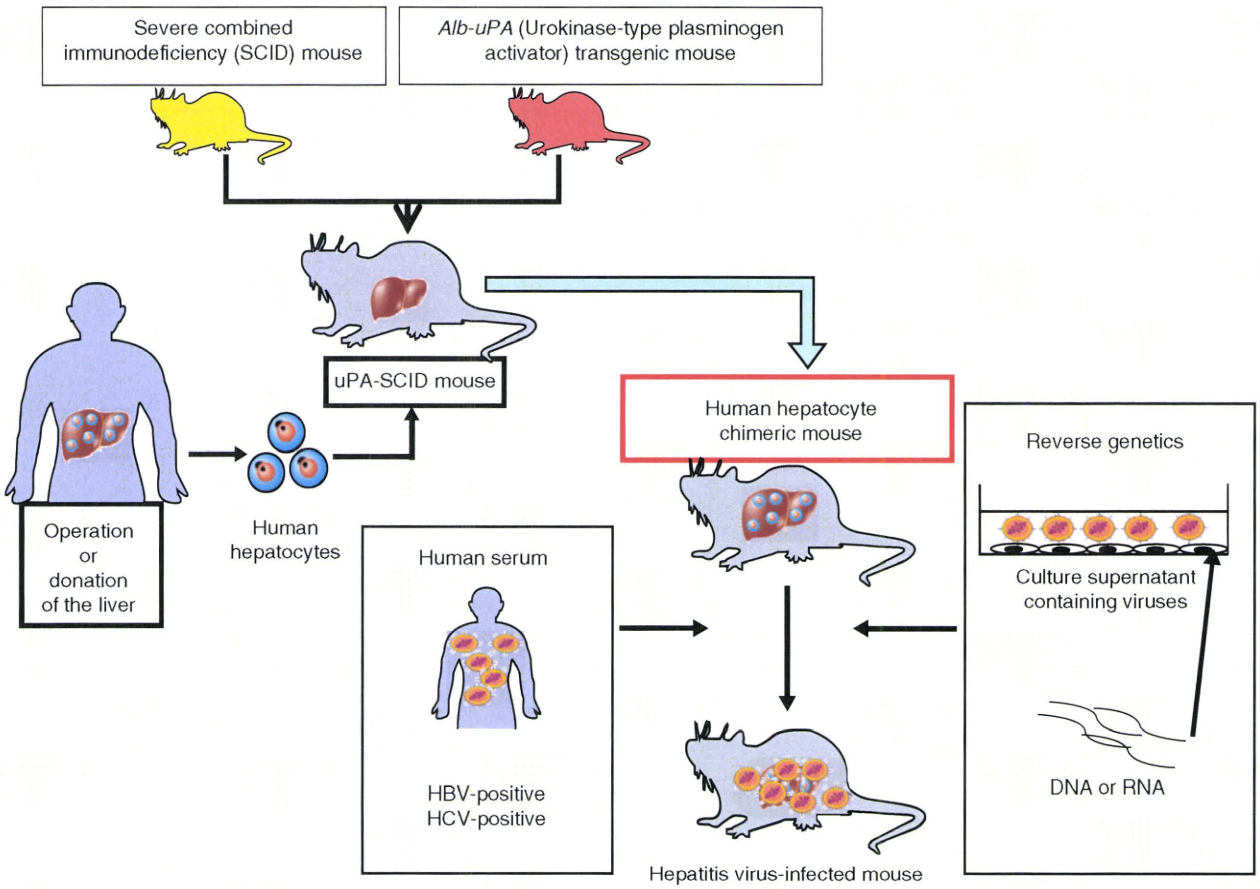

Figure 1 Generation of human hepatocyte chimeric mice and hepatitis virus infection model. A uPA/scid mouse was created by mating uPA transgenic mouse and scid mouse. Human hepatocytes obtained by surgical resection or donation were transplanted to newborn mice. The chimeric mice can be infected with hepatitis B virus (HBV) or hepatitis C (HBC) virus by injecting human serum containing these viruses. Alternatively, the mice can be infected by HBV[13] or HCV[14] created in cell culture or by injecting HCV RNA into the mouse liver.[15]

are susceptible to infection with both HBV and HCV, and as such comprised the most effective small animal model for chronic hepatitis so far developed.[19,20] An example of a highly repopulated mouse liver that we are using in experiments is shown in Figure 2.

Highly repopulated mice have been shown to be a valuable model for the study of drug metabolism.[21–29] Advances in technology for human hepatocyte transplantation have enabled serial passage of human hepatocytes in uPA/scid mice and have been shown to retain infectivity for HBV.[30]

This mouse model and other animal models for the study of hepatitis viruses have been summarized in reviews by Meuleman and Leroux-Roels,[31] Dandri *et al.*,[32,33] Barth *et al.*,[34] and Kneteman and Toso.[35] The present review will focus on key issues and updated information.

Study of hepatitis B virus infection using human hepatocyte chimeric mice

Since the initial reports of successful transmission of HBV to human hepatocyte chimeric mice in 2001 and 2004,[16,27] several researchers have reported transmission of HBV into similar mice.[13,36,37] In these studies, passage experiments studies show that HBV replicating in mice retain infectivity.[13,36] Further, the presence of viral proteins has been shown immunohistochemically in human hepatocytes transplanted into mouse livers, but these are not present in mouse hepatocytes.[13,36,37] Formation of viral particles in infected mouse livers can be shown by electron microscopy.[36,37] Genetically engineered viruses lacking HBe-antigen have also been shown to infect chimeric mice, proving that e antigen is dispensable for viral infection and replication.[13] In contrast, HBx protein has been shown to be indispensable for viral replication.[38] Transcomplementation of HBx protein with hydrodynamic injection restored HBV infectivity in mice. Interestingly, all revertant viruses show a restored ability to express HBx.[38]

By infecting chimeric mice with genotype A, B and C, differing proliferative capacity has been shown between HBV genotypes.[37] In mice infected for a relatively short time, there are no morphological changes in HBV infected mice livers in studies.[13,36] In contrast, the occurrence of liver cell damage has been reported after long-term infection of chimeric mice with HBV[39] or with specific strains of HBV;[40] these findings are consistent with direct cytopathic effects of HBV under certain conditions.

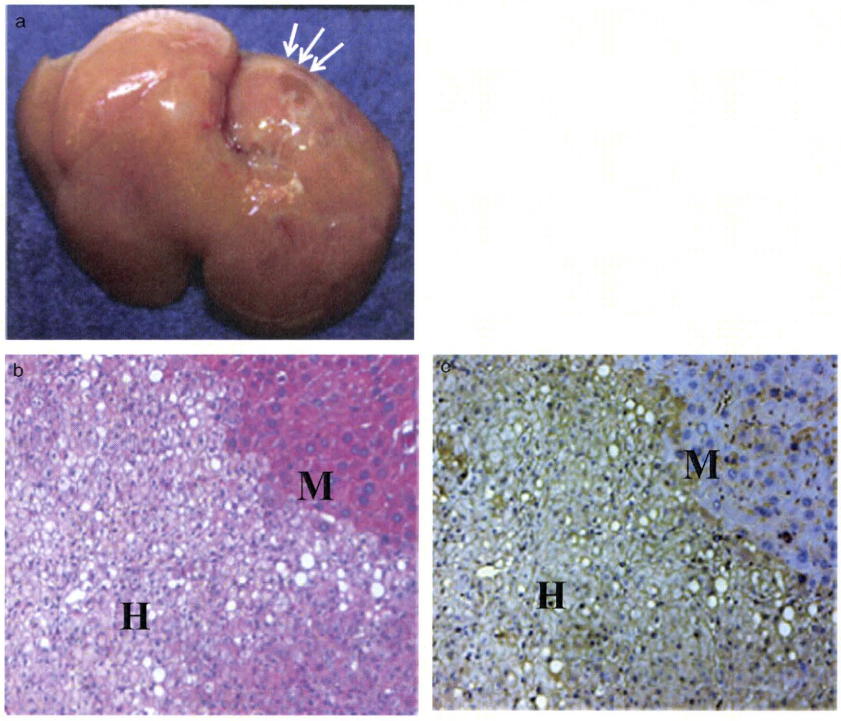

Figure 2 Representative uPA/scid mouse livers repopulated by human hepatocytes. (a) Mouse liver almost completely repopulated by human hepatocytes. Only a small portion of mouse hepatocytes are shown by arrows. (b) Microscopic figure of the mouse liver. M and H indicate regions consisting of mouse and human hepatocytes, respectively (Hematoxylin–eosin staining, magnification: ×100). (c) Microscopic figure of the mouse liver stained with antibody directed against human serum albumin.

The biological properties of a newly identified unique strain of HBV, genotype G, which replicates only in the presence of another genotype, were confirmed using the chimeric mouse.[41] Infectivity of another novel HBV strain, identified from a Japanese patient, that is divergent from known human and ape HBV has also been confirmed.[42] Titration of HBV infectivity, which previously could only be carried out using chimpanzees, can be carried out effectively using chimeric mice.[43]

Taking advantage of the absence of human immune cells in the chimeric mice, Noguchi *et al.*[44] showed that hypermutation of HBV increases in human hepatocytes under interferon treatment. Dandri *et al.* measured viral half-life in human and chimeric mice repopulated with wooly monkey hepatocytes.[45] The results clearly showed that viral half-life is shortened by immunological mechanisms in humans with low viral levels, but not in chimeric mice where functional immunity is absent. Hiraga *et al.*[46] showed an absence of interference between HBV and HCV.

Evaluation of therapeutic agents is the most important role for this mouse model. Tsuge *et al.*[13] assessed the effect of interferon and lamivudine using chimeric mice. Similarly, Dandri *et al.*[47] showed the effects of adefovir using uPA/scid mice repopulated with tupaia hepatocytes, which also support replication of human HBV. Oga *et al.*[48] identified a novel lamivudine-resistant variant that has an amino acid substitution outside of the YMDD motif. They showed that lamivudine was ineffective against the novel mutant strain. It is thus apparent that this mouse/human liver chimeric model is ideal to study the susceptibility of mutant strains to various drugs, because mutant viruses can easily be made and infected into chimeric mice.[13] The model has also been utilized to evaluate viral entry inhibitors derived from the large envelope protein.[49]

Study of hepatitis C virus using human hepatocyte chimeric mice

As observed in studies on HBV, HCV infection efficiency was poor and levels of viremia were low in mice where the repopulation rate of the mouse liver with human hepatocyte was low.[17,50] As shown in Figure 3, human albumin levels in mouse serum were significantly higher in mice in which measurable viremia developed (Hiraga *et al.* unpublished data). Recent studies have therefore been carried out using highly repopulated mice. The usefulness of a newly developed HCV assay,[51] and infectivity of a newly identified intergenotypic recombinant strain,[52] have been reported using the chimeric mice.

Using the remarkable replication ability of the JFH1 genotype 2a strain,[53] infectivity of JFH1 or intergenotypic chimeric viral particles, previously shown in cell culture, has now been shown to be infectious in chimeric mice.[54–56] Infectivity of viruses that were replicated in chimeric mice in cell culture has also been shown, and virus fitness has been studied.[55,56] The role of the HCV core+1 open reading frame and core *cis*-acting RNA elements has also been examined using the chimeric virus.[57] These elegant studies have the limitation that the non-structural part of the virus is limited to that of JFH1. Hiraga *et al.*[14] have shown that infectious clones of genotype 1a and JFH1 can be infected with direct injection of *in vitro* transcribed RNA into the mouse liver.[14] Similarly, Kimura *et al.*[15] reported the establishment of infectious clones of genotype 1b and ablation of RNA polymerase by site-directed mutagenesis abolish infectivity. These infectious clones will be useful for the study of drug-resistant strains.

The model of HCV infection has also been used to show that infection of the virus can be prevented by antibodies against

Table 1 New therapeutic strategies tested by human hepatocyte chimeric mice

n	Drug or cell	Strategy	Reference
1	Interferon alpha 2b	Activation of antiviral genes	Kneteman *et al.*[65]
	BILN-2061	NS3-4A protease inhibition	
	HCV371	NS5B polymerase inhibition	
2	Modified BID	Induction of apoptosis	Hsu *et al.*[66]
3	Serine palmitoyltransferase inhibitor	Disruption of lipid raft	Umehara *et al.*[67]
4	Lymphoblastoid interferon alpha	Activation of antiviral genes	Hiraga *et al.*[14]
5	Amphipathic DNA polymers	Blocking viral entry	Matsumura *et al.*[60]
6	Sec-butyl-analogue of HCV-371	NS5B polymerase inhibition	LaPorte *et al.*[68]
7	HCV796	NS5B polymerase inhibition	Kneteman *et al.*[69]
8	Liver allograft-derived lymphocyte	Adoptive immunotherapy	Ohira *et al.*[70]
9	Telaprevir	NS3-4A protease inhibition	Kamiya *et al.*[71]

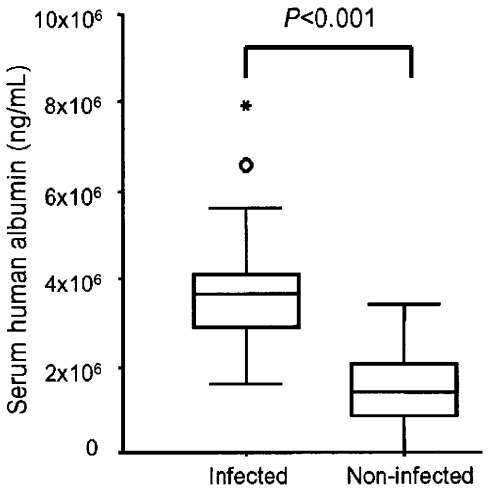

Figure 3 Human albumin levels in mice used in the hepatitis C virus (HCV) infection experiments. A total of 54 mice were injected with HCV positive serum samples containing 5×10^5 virus particles. A total of 24 mice became persistently positive for HCV-RNA, but 30 mice did not. Serum human albumin levels 2 weeks after human hepatocyte transplantation were compared between infected and non-infected mice.

CD81,[58] polyclonal human immunoglobulin directed to a similar strain,[59] and amphipathic DNA polymers.[60] Notably, the presence of broadly neutralizing antibodies to HCV that protect against heterologous viral infection has been reported, suggesting the possibility of a prophylactic vaccine against HCV.[61]

With respect to evasion of the virus against the innate immune response, altered intrahepatic expression profiles in the early phase of infection is of particular interest. The chimeric mice model is ideal for such studies; cross-hybridization of mouse and human can be avoided by careful experimental procedures.[62] Microarray analysis of livers of HCV infected and non-infected mice showed transcriptional activation of genes related to innate immune response, lipid metabolism, endoplasmic reticulum (ER) stress and apoptosis in HCV-infected mice.[63,64] The HCV infected mouse model is particularly useful for the study of newly developed HCV agents. The effect of recently developed chemicals and a unique therapy using intrahepatic lymphocytes have been shown using this model (Table 1). However, none of these therapies have yet been able to completely eradicate HCV from mice. It is noteworthy that ultra-rapid cardiotoxicity has been reported with the protease inhibitor BILN 2061 in the uPA/scid mice, but not in scid mice, implicating involvement of the uPA transgene.[72] Care should therefore be taken in interpreting the results obtained by this model.

Conclusion

Development of a small animal model using human hepatocyte chimeric mice has enabled us to study key aspects of HBV and HCV biology. The characteristic feature of the absence of human immune cells is suitable for studying viral replication and observing changes occurring in liver cells during viral infection, such as the innate immune response and cellular stress and metabolic responses. The model is also useful for studying the effect of drugs without the influence of cytokines and cytotoxic T lymphocytes. Nonetheless, the model is insufficient to study carcinogenesis of hepatitis viruses, because non-parenchymal cells in mouse liver are of mouse origin and do not support inflammation and fibrosis, which are probably closely related to carcinogenesis. The lack of human immune cells also limits the study of inflammation and immunity. Furthermore, the availability of human hepatocytes is limited. Despite these limitations, the current model shows great potential as a mouse model for the study of hepatitis viruses. Development of a small animal model with or without human immunity using stem cells or iPS cells would be an ideal model in the future.

Acknowledgments

This work was supported in part by Grants-in-Aid for scientific research and development from the Ministry of Education, Culture, Sports, Science and Technology, and the Ministry of Health, Labor and Welfare, Government of Japan.

References

1 Shepard CW, Simard EP, Finelli L, Flore AE, Bell BP. Hepatitis B virus infection: epidemiology and vaccination. *Epidemiol. Rev.* 2006; **28**: 112–25.

2 Sy T, Jamal MM. Epidemiology of Hepatitis C Virus (HCV) infection. *Int. J. Med. Sci.* 2006; **3**: 41–6.
3 Yuen MF, Hou JL, Chutaputti A, Prevent APWP. Hepatocellular carcinoma in the Asia pacific region. *J. Gastroenterol. Hepatol.* 2009; **24**: 346–53.
4 Guidotti LG, Matzke B, Schaller H, Chisari FV. High-level Hepatitis-B Virus-replication in transgenic mice. *J. Virol.* 1995; **69**: 6158–69.
5 Weber O, Schlemmer KH, Hartmann E *et al.* Inhibition of human hepatitis B virus (HBV) by a novel non-nucleosidic compound in a transgenic mouse model. *Antiviral Res.* 2002; **54**: 69–78.
6 Julander JG, Sidwell RW, Morrey JD. Characterizing antiviral activity of adefovir dipivoxil in transgenic mice expressing hepatitis B virus. *Antiviral Res.* 2002; **55**: 27–40.
7 Julander JG, Colonno RJ, Sidwell RW, Morrey JD. Characterization of antiviral activity of entecavir in transgenic mice expressing hepatitis B virus. *Antiviral Res.* 2003; **59**: 155–61.
8 Uprichard SL, Boyd B, Althage A, Chisari FV. Clearance of hepatitis B virus from the liver of transgenic mice by short hairpin RNA. *Proc. Natl. Acad. Sci U S A* 2005; **102**: 773–8.
9 Ilan E, Burakova T, Dagan S *et al.* The hepatitis B virus-trimera mouse: a model for human HBV infection and evaluation of Anti-HBV therapeutic agents. *Hepatology* 1999; **29**: 553–62.
10 Ilan E, Arazi J, Nussbaum O *et al.* The hepatitis C virus (HCV)-Trimera mouse: a model for evaluation of agents against HCV. *J. Infect. Dis.* 2002; **185**: 153–61.
11 Heckel JL, Sandgren EP, Degen JL, Palmiter RD, Brinster RL. Neonatal bleeding in transgenic mice expressing urokinase-type plasminogen-activator. *Cell* 1990; **62**: 447–56.
12 Rhim JA, Sandgren EP, Palmiter RD, Brinster RL. Complete reconstitution of mouse-liver with xenogeneic hepatocytes. *Proc. Natl. Acad Sci U S A* 1995; **92**: 4942–6.
13 Tsuge M, Hiraga N, Takaishi H *et al.* Infection of human hepatocyte chimeric mouse with genetically engineered hepatitis B virus. *Hepatology* 2005; **42**: 1046–54.
14 Hiraga N, Imamura M, Tsuge M *et al.* Infection of human hepatocyte chimeric mouse with genetically engineered Hepatitis C Virus and its susceptibility to interferon. *FEBS Lett.* 2007; **581**: 1983–7.
15 Kimura T, Imamura M, Hiraga N *et al.* Establishment of an infectious genotype 1b Hepatitis C Virus clone in human hepatocyte chimeric mice. *J.l Gen. Virol.* 2008; **89**: 2108–13.
16 Dandri M, Burda MR, Torok E *et al.* Repopulation of mouse liver with human hepatocytes and in vivo infection with hepatitis B virus. *Hepatology* 2001; **33**: 981–8.
17 Mercer DF, Schiller DE, Elliott JF *et al.* Hepatitis C virus replication in mice with chimeric human livers. *Nat. Med.* 2001; **7**: 927–33.
18 Douglas DN, Kawahara T, Sis B *et al.* therapeutic efficacy of human hepatocyte transplantation in a SCID/uPA mouse model with inducible liver disease. *PLoS ONE* 2010; **5**: e9209.
19 Tateno C, Yoshizane Y, Saito N *et al.* Near completely humanized liver in mice shows human-type metabolic responses to drugs. *Am. J. Pathol.* 2004; **165**: 901–12.
20 Bissig KD, Wieland SF, Tran P *et al.* Human liver chimeric mice provide a model for hepatitis B and C virus infection and treatment. *J. Clin. Invest.* 2010; **120**: 924–30.
21 Yu AM, Idle JR, Gonzalez FJ. Polymorphic cytochrome p450 2D6: humanized mouse model and endogenous substrates. *Drug. Metab. Rev.* 2004; **36**: 243–77.
22 Katoh M, Sawada T, Soeno Y *et al.* In vivo drug metabolism model for human cytochrome P450 enzyme using chimeric mice with humanized liver. *J. Pharm. Sci.-Us.* 2007; **96**: 428–37.
23 Katoh M, Matsui T, Nakajima M *et al.* In vivo induction of human cytochrome P450 enzymes expressed in chimeric mice with humanized liver. *Drug. Metab. Dispos.* 2005; **33**: 754–63.
24 Katoh M, Matsui T, Okumura H *et al.* Expression of human phase II enzymes in chimeric mice with humanized liver. *Drug. Metab. Dispos.* 2005; **33**: 1333–40.
25 Okumura H, Katoh M, Sawada T *et al.* Humanization of excretory pathway in chimeric mice with humanized liver. *Toxicol. Sci.* 2007; **97**: 533–8.
26 Shoda J, Okada K, Inada Y *et al.* Bezafibrate induces multidrug-resistance P-Glycoprotein 3 expression in cultured human hepatocytes and humanized livers of chimeric mice. *Hepatol. Res.* 2007; **37**: 548–56.
27 Petersen J, Burda MR, Dandri M, Rogler CE. Transplantation of human hepatocytes in immunodeficient UPA mice: a model for the study of hepatitis B virus. *Methods Mol. Med.* 2004; **96**: 253–60.
28 Yoshizato K, Tateno C. A human hepatocyte-bearing mouse: an animal model to predict drug metabolism and effectiveness in humans. *PPAR Res.* 2009; **2009**: 476217.
29 Yoshizato K, Tateno C, Utoh R. The mechanism of liver size control in mammals: a novel animal study. *Int. J. Design & Nature Ecodynamics* 2009; **4**: 123–42.
30 Utoh R, Tateno C, Yamasaki C *et al.* Susceptibility of chimeric mice with livers repopulated by serially subcultured human hepatocytes to hepatitis B virus. *Hepatology* 2008; **47**: 435–46.
31 Meuleman P, Leroux-Roels G. The human liver-uPA-SCID mouse: a model for the evaluation of antiviral compounds against HBV and HCV. *Antiviral Res.* 2008; **80**: 231–8.
32 Dandri M, Lutgehetmann M, Volz T, Petersen J. Small animal model systems for studying Hepatitis B Virus replication and pathogenesis. *Semin. Liver Dis.* 2006; **26**: 181–91.
33 Dandri M, Volz TK, Lutgehetmann M, Petersen J. Animal models for the study of HBV replication and its variants. *J. Clin. Virol.* 2005; **34** (Suppl. 1): S54–62.
34 Barth H, Robinet E, Liang TJ, Baumert TF. Mouse models for the study of HCV infection and virus-host interactions. *J. Hepatol.* 2008; **49**: 134–42.
35 Kneteman NM, Toso C. In vivo study of HCV in mice with chimeric human livers. *Methods Mol. Biol.* 2009; **510**: 383–99.
36 Meuleman P, Libbrecht L, De Vos R *et al.* Morphological and biochemical characterization of a human liver in a uPA-SCID mouse chimera. *Hepatology* 2005; **41**: 847–56.
37 Sugiyama M, Tanaka Y, Kato T *et al.* Influence of hepatitis B virus genotypes on the intra- and extracellular expression of viral DNA and antigens. *Hepatology* 2006; **44**: 915–24.
38 Tsuge M, Hiraga N, Akiyama R *et al.* HBx protein is indispensable for development of viremia in human hepatocyte chimeric mice. *J. Gen. Virol.* 2010.
39 Meuleman P, Libbrecht L, Wieland S *et al.* Immune suppression uncovers endogenous cytopathic effects of the hepatitis B virus. *J. Virol.* 2006; **80**: 2797–807.
40 Sugiyama M, Tanaka Y, Kurbanov F *et al.* Direct cytopathic effects of particular hepatitis B virus genotypes in severe combined immunodeficiency transgenic with urokinase-type plasminogen activator mouse with human hepatocytes. *Gastroenterology* 2009; **136**: 652–62.
41 Tanaka Y, Sanchez LV, Sugiyama M *et al.* Characteristics of Hepatitis B Virus genotype G coinfected with genotype H in chimeric mice carrying human hepatocytes. *Virology* 2008; **376**: 408–15.
42 Tatematsu K, Tanaka Y, Kurbanov F *et al.* A genetic variant of Hepatitis B Virus divergent from known human and ape genotypes isolated from a Japanese patient and provisionally assigned to new genotype J. *J. Virol.* 2009; **83**: 10538–47.
43 Tabuchi A, Tanaka J, Katayama K *et al.* Titration of Hepatitis B Virus infectivity in the sera of pre-acute and late acute phases of HBV infection: transmission experiments to chimeric mice with

human liver repopulated hepatocytes. *J. Med. Virol.* 2008; **80**: 2064–8.
44 Noguchi C, Imamura M, Tsuge M *et al.* G-to-A Hypermutation in Hepatitis B Virus (HBV) and clinical course of patients with chronic HBV infection. *J. Infect. Dis.* 2009; **199**: 1599–607.
45 Dandri M, Murray JM, Lutgehetmann M, Volz T, Lohse AW, Petersen J. Virion half-life in chronic hepatitis B infection is strongly correlated with levels of viremia. *Hepatology* 2008; **48**: 1079–86.
46 Hiraga N, Imamura M, Hatakeyama T *et al.* Absence of viral interference and different susceptibility to interferon between Hepatitis B Virus and Hepatitis C Virus in human hepatocyte chimeric mice. *J. Hepatol.* 2009; **51**: 1046–54.
47 Dandri M, Burda MR, Zuckerman DM *et al.* Chronic infection with Hepatitis B Viruses and antiviral drug evaluation in uPA mice after liver repopulation with tupaia hepatocytes. *J. Hepatol.* 2005; **42**: 54–60.
48 Yatsuji H, Noguchi C, Hiraga N *et al.* Emergence of a novel lamivudine-resistant hepatitis B virus variant with a substitution outside the YMDD motif. *Antimicrob. Agents Chemother.* 2006; **50**: 3867–74.
49 Petersen J, Dandri M, Mier W *et al.* Prevention of Hepatitis B Virus infection in vivo by entry inhibitors derived from the large envelope protein. *Nat. Biotechnol.* 2008; **26**: 335–41.
50 Turrini P, Sasso R, Germoni S *et al.* Development of humanized mice for the study of hepatitis C virus infection. *Transplant. Proc.* 2006; **38**: 1181–4.
51 Cagnon L, Wagaman P, Bartenschlager R *et al.* Application of the trak-C (TM) HCV core assay for monitoring antiviral activity in HCV replication systems. *J. Virol. Methods* 2004; **118**: 23–31.
52 Kurbanov F, Tanaka Y, Chub E *et al.* Molecular epidemiology and interferon susceptibility of the natural recombinant Hepatitis C Virus Strain RF1-2k/1b. *J. Infect. Dis.* 2008; **198**: 1448–56.
53 Wakita T, Pietschmann T, Kato T *et al.* Production of infectious hepatitis C virus in tissue culture from a cloned viral genome. *Nat. Med.* 2005; **11**: 791–6.
54 Grove J, Huby T, Stamataki Z *et al.* Scavenger receptor BI and BII expression levels modulate Hepatitis C Virus infectivity. *J. Virol.* 2007; **81**: 3162–9.
55 Lindenbach BD, Meuleman P, Ploss A *et al.* Cell culture-grown Hepatitis C Virus is infectious in vivo and can be recultured in vitro. *Proc. Natl. Acad. Sci. U S A* 2006; **103**: 3805–9.
56 Kaul A, Woerz I, Meuleman P, Leroux-Roels G, Bartenschlager R. Cell culture adaptation of Hepatitis C Virus and in vivo viability of an adapted variant. *J. Virol.* 2007; **81**: 13168–79.
57 Vassilaki N, Friebe P, Meuleman P *et al.* Role of the Hepatitis C Virus Core+1 open reading frame and core cis-acting RNA Elements in Viral RNA translation and replication. *J. Virol.* 2008; **82**: 11503–15.
58 Meuleman P, Hesselgesser J, Paulson M *et al.* Anti-CD81 antibodies can prevent a Hepatitis C Virus infection in vivo. *Hepatology* 2008; **48**: 1761–8.
59 Vanwolleghem T, Bukh J, Meuleman P *et al.* Polyclonal immunoglobulins from a chronic Hepatitis C Virus patient protect human liver-chimeric mice from infection with a homologous Hepatitis C Virus strain. *Hepatology* 2008; **47**: 1846–55.
60 Matsumura T, Hu ZY, Kato T *et al.* Amphipathic DNA polymers inhibit Hepatitis C Virus infection by blocking viral entry. *Gastroenterology* 2009; **137**: 673–81.
61 Law M, Maruyama T, Lewis J *et al.* Broadly neutralizing antibodies protect against Hepatitis C Virus quasispecies challenge. *Nat. Med.* 2008; **14**: 25–7.
62 Walters KA, Joyce MA, Thompson JC *et al.* Application of functional genomics to the chimeric mouse model of HCV infection: optimization of microarray protocols and genomics analysis. *Virol. J.* 2006; **3**: 37–44.
63 Walters KA, Joyce MA, Thompson JC *et al.* Host-specific response to HCV infection in the chimeric SCID-beige/Alb-uPA mouse model: role of the innate antiviral immune response. *PLoS Pathog.* 2006; **2**: 591–602.
64 Joyce MA, Walters KA, Lamb SE *et al.* HCV Induces Oxidative and ER Stress, and Sensitizes Infected Cells to Apoptosis in SCID/Alb-uPA Mice. *PLoS Pathog.* 2009; **5**: e10000291.
65 Kneteman NM, Weiner AJ, O'Connell J *et al.* Anti-HCV therapies in chimeric scid-Alb/uPA mice parallel outcomes in human clinical application. *Hepatology* 2006; **43**: 1346–53.
66 Hsu EC, Hsi B, Hirota-Tsuchihara M *et al.* Modified apoptotic molecule (BID) reduces hepatitis C virus infection in mice with chimeric human livers. *Nat. Biotechnol.* 2003; **21**: 519–25.
67 Umehara T, Sudoh M, Yasui F *et al.* Serine palmitoyltransferase inhibitor suppresses HCV replication in a mouse model. *Biochem. Biophys. Res. Commun.* 2006; **346**: 67–73.
68 Laporte MG, Jackson RW, Draper TL *et al.* The discovery of pyrano[3,4-b]indole-based allosteric inhibitors of HCV NS5B polymerase with in vivo activity. *Med. Chem.* 2008; **3**: 1508–15.
69 Kneteman NM, Howe AYM, Gao TJ *et al.* HCV796: a selective nonstructural protein 5B polymerase inhibitor with potent Anti-Hepatitis C Virus activity in vitro, in mice with chimeric human livers, and in humans infected with Hepatitis C Virus. *Hepatology* 2009; **49**: 745–52.
70 Ohira M, Ishiyama K, Tanaka Y *et al.* Adoptive immunotherapy with liver allograft-derived lymphocytes induces anti-HCV activity after liver transplantation in humans and humanized mice. *J. Clin. Invest.* 2009; **119**: 3226–35.
71 Kamiya N, Iwao E, Hiraga N *et al.* Practical Evaluation of a Mouse with Chimeric Human Liver Model for Hepatitis C Virus Infection Using an NS3-4A Protease Inhibitor. *J. Gen. Virol.* 2010; **91**: 1668–77.
72 Vanwolleghem T, Meuleman P, Libbrecht L *et al.* Ultra-rapid cardiotoxicity of the hepatitis C virus protease inhibitor BILN 2061 in the urokinase-type plasminogen activator mouse. *Gastroenterology* 2007; **133**: 1144–55.

HCV substitutions and IL28B polymorphisms on outcome of peg-interferon plus ribavirin combination therapy

C Nelson Hayes,[1,2] Mariko Kobayashi,[3] Norio Akuta,[3] Fumitaka Suzuki,[3] Hiromitsu Kumada,[3] Hiromi Abe,[1,2] Daiki Miki,[1,2] Michio Imamura,[1,2] Hidenori Ochi,[1,2] Naoyuki Kamatani,[4] Yusuke Nakamura,[5] Kazuaki Chayama[1,2]

[1]Laboratory for Digestive Diseases, Center for Genomic Medicine, RIKEN, Hiroshima, Japan
[2]Department of Medicine and Molecular Science, Division of Frontier Medical Science, Programs for Biomedical Research, Graduate School of Biomedical Sciences, Hiroshima University, Hiroshima, Japan
[3]Department of Hepatology, Toranomon Hospital, Tokyo, Japan
[4]Center for Genomic Medicine, Riken, Yokohama, Japan
[5]Laboratory of Molecular Medicine, Human Genome Center, The Institute of Medical Science, University of Tokyo, Tokyo, Japan

Correspondence to
Professor Kazuaki Chayama, Department of Medical and Molecular Science, Division of Frontier Medical Science, Programs for Biomedical Research, Graduate School of Biomedical Science, Hiroshima University, 1-2-3 Kasumi, Minami-ku, Hiroshima 734-8551, Japan; chayama@hiroshima-u.ac.jp

Revised 21 September 2010
Accepted 26 September 2010
Published Online First 10 November 2010

ABSTRACT

Background and aims A number of recent studies have shown that human polymorphisms near the *IL28B* type III interferon (IFNλ) gene influence the response to peg-interferon plus ribavirin combination therapy for infection with chronic hepatitis C virus (HCV). Viral polymorphisms, including substitutions within the HCV core and NS5A proteins, have also been shown to influence treatment outcome, but it is not known whether these factors act independently of the IL28B polymorphism or if they reflect the same or a different underlying mechanism. Multiple logistic regression was used to determine whether host and viral polymorphisms independently predict sustained virological response (SVR).

Methods Two single nucleotide polymorphisms were genotyped in the IL28B locus (rs12979860 and rs8099917) from 817 patients with chronic HCV infection, and substitutions at amino acids 70 and 91 of the HCV core protein and within the NS5A interferon sensitivity-determining region (ISDR) were analysed.

Results It was found that independent predictors of an SVR included IL28B rs12979860 CC genotype (OR=4.98; p=4.00E-08), core amino acid 70 substitutions (OR=0.53; p=0.016), age and baseline viral load. For non-virological response, the IL28B rs12979860 CT/TT genotype (OR=0.23; p=1.96E-8) and age were independent predictors. IL28B rs12979860 genotype (p=1.4E-8), core amino acid 70 substitutions (p=0.0013), ISDR substitutions (p=0.0019), baseline viral load, γ-glutamyltranspeptidase, alanine aminotransferase and platelet count were independent predictors for change in viral load by week 4 of treatment.

Conclusions IL28B polymorphisms and HCV core amino acid 70 substitutions contribute independently to an SVR to peg-interferon plus ribavirin combination therapy.

Significance of this study

What is already known about this subject?

- Clinical and viral factors influence the outcome of peg-interferon plus ribavirin combination therapy for chronic hepatitis C virus infection.
- Polymorphisms within the human IL28B locus strongly influence treatment outcome.
- Substitutions at amino acids 70 and 91 of the HCV core protein as well as within the interferon sensitivity-determining region (ISDR) also affect response to treatment.

What are the new findings?

- IL28B polymorphisms as well as substitutions at amino acid 70 both independently predict sustained virological response, suggesting that they influence treatment outcome through different mechanisms.
- IL28B polymorphisms, substitutions at core protein amino acid 70 and ISDR substitutions are each independent predictors for change in viral load after 4 weeks of treatment.

How might it impact on clinical practice in the forseeable future?

- The combination of IL28B genotyping and detection of core protein substitutions may yield more accurate pretreatment predictions of treatment efficacy.

INTRODUCTION

Hepatitis C virus (HCV) is a primary cause of chronic hepatitis and often progresses to liver cirrhosis and hepatocellular carcinoma.[1 2] Peg-interferon plus ribavirin combination therapy (PEG-RBV) is the current standard of care, but it is only effective in 50% of patients and has severe side effects often requiring discontinuation or dose modification.[3] Consequently, reliable predictors are needed to identify unsuitable candidates as early as possible.

Genome-wide association studies have reported common single nucleotide polymorphisms (SNPs) predictive of response to interferon treatment. While polymorphisms in MxA,[4 5] interferon α-receptor 1,[6] osteopontin[7] and MAPKAPK3[8] have been reported to be associated with interferon response, several linked SNPs within the IL28B locus on chromosome 19 have recently been shown to be the strongest predictors of early viral kinetics, response to treatment and spontaneous viral clearance.[9–15]

Viral polymorphisms have also been shown to be associated with treatment response. HCV genotypes 1 and 4 in particular are considered more difficult to treat than genotypes 2 and 3,[16 17] and genotype 3 is associated with steatosis.[18] Within genotype 1b, amino acid substitutions at positions 70 and 91 of the HCV core protein and accumulation of substitutions in the interferon sensitivity-determining region (ISDR) of the NS5A protein[19 20] have also been shown to be associated with treatment outcome, especially among Japanese patients.

Consequently, a number of human and viral factors are now known to affect response to treatment, but in order to identify the most important independent predictors and to identify which, if any, may be useful in guiding clinical practice, it is necessary to analyse them simultaneously in a multivariate model. In this study we therefore attempted to identify host and viral factors that independently predict treatment outcome.

MATERIALS AND METHODS

Patients

Data from 817 patients who were treated with PEG-RBV combination therapy for chronic hepatitis C genotype 1b infection between 2002 and 2008 were collected from Toranomon Hospital (Tokyo) and hospitals that belong to the Hiroshima Liver Study Group (http://home.hiroshima-u.ac.jp/naika1/hepatology/english/study.html) in Hiroshima, Japan. Study subjects tested positive for HCV RNA over a span of >6 months, were negative for hepatitis B and HIV, and showed no evidence of other liver diseases. Patients received weekly injections of peg-interferon-α2b at 1.5 g/kg body weight for 48 weeks and ribavirin was administered orally. The amount of ribavirin was adjusted based on body weight (600 mg for <60 kg, 800 mg for 60–80 kg, 1000 mg for >80 kg). Patients with low baseline viral load (<5 log IU/ml) were excluded, as were patients who received <0.89 g/kg of peg-interferon or <8.3 mg/kg of ribavirin. Treatment success was evaluated based on a sustained virological response (SVR), defined as undetectable HCV RNA levels 24 weeks after cessation of treatment. Some patients showed a transient response (TR or relapser), in which HCV RNA dropped to undetectable levels during treatment but then later rebounded. In those with a non-viral response (NVR), HCV RNA levels failed to decline by 2 log10 IU/ml by week 12 of treatment and never dropped below detectable levels. Histopathological diagnosis was made according to the criteria of Desmet *et al.*[21] All subjects gave written informed consent to participate in the study according to the process approved by the ethical committee of each hospital and conforming to the ethical guidelines of the 1975 Declaration of Helsinki.

HCV RNA levels

HCV RNA levels were monitored throughout the course of treatment at 1 or 2 month intervals for a total of at least six time points via reverse transcription–PCR (RT–PCR) using the original Amplicor method, the high range method or the TaqMan RT–PCR test. The measurement ranges of these assays were 0.5–850 kIU/ml, 5–5000 kIU/ml and 1.2–7.8 log IU, respectively. Samples exceeding the measurement range were diluted with phosphate-buffered saline (PBS) and reanalysed. All values were reported as log IU/ml.

ISDR and core amino acid substitutions

Amino acid substitutions in the HCV core and ISDRs were determined by direct sequencing of PCR products following extraction and reverse transcription of serum HCV RNA. Core amino acid substitutions at positions 70 and 91 (core70 and core91) were determined according to Akuta *et al*,[22 23] and the number of ISDR substitutions was established as in Enomoto *et al.*[19 21 24] Of the 817 patients in the study, substitutions for both ISDR and core70 could be determined for 379 patients.

SNP genotyping

We genotyped each patient for two IL28B SNPs previously reported to be associated with treatment outcome, rs12979860 and rs8099917.[9–11] Samples were genotyped using the Illumina HumanHap610-Quad Genotyping BeadChip or the Invader assay, as described previously.[25 26] The two SNPs are in strong linkage disequilibrium, with a correlation coefficient of 0.99. SNP genotypes for both rs12979860 and rs8099917 were determined for 815 patients (99.7%).

Statistical analysis

All analyses were performed using the R statistical package (http://www.r-project.org). Non-parametric tests (χ^2 and Mann–Whitney U tests) were used to detect significant associations. All statistical analyses were two sided, and $p<0.05$ was considered significant. Simple and multiple logistic regression analyses were used to examine the association between viral substitutions and clinical factors using $p<0.05$ as the criterion for inclusion in the initial multivariate model. Multivariate logistic regression analysis was performed using forward/backward stepwise selection based on Akaike Information Criterion (AIC) score and validated using the rms package in R. ORs and 95% CIs were calculated for each factor.

RESULTS

Patient characteristics

Patient profiles are shown in table 1. Forty-five per cent of patients achieved an SVR, 22% were transient responders and 33% failed to respond to treatment (NVR). Males were significantly more likely to achieve an SVR than females (50% and 38%, respectively; p=0.0011), and younger patients were more likely to achieve an SVR than older patients (59.2% and 40.9% above and below median age 58, respectively; p=1.57E-6). Patients who achieved an SVR also had lower γ-glutamyltranspeptidase (γGTP) levels (36 IU/l vs 45 IU/l; p= 0.008) and higher platelet counts (17.1 vs 15.3×10^{10}/L; p=3.649E-05) than those who did not.

IL28B SNP genotypes

The genotypes of two IL28B SNPs were measured for each patient. Because of linkage disequilibrium, SNP results are nearly interchangeable. However, six patients showed an intermediate haplotype consisting of the favourable genotype for rs8099917 (TT) but an unfavourable genotype for rs12979860 (CT), whereas only one of the six patients achieved an SVR, suggesting that rs12979860 is a better predictor of SVR in this data set.

The frequency of the risk allele (T) for rs12979860 was 0.15 among all patients and 0.08 in SVR patients, 0.14 in TR patients and 0.27 in NVR patients. Patients homozygous for the rs12979860 favourable allele (CC) were significantly more likely to achieve an SVR compared with those with TC or TT genotypes (53% vs 24%, OR=3.55, p=3.95E-13). Conversely, patients with the risk allele (TC or TT) were significantly more likely to show an NVR (55% vs 25%; OR=0.265; p=4.4E-16). Patients with the rs12979860 CC genotype had a marginally lower baseline viral load (6.6 vs 6.4 log IU/ml; p=0.093), but showed significantly greater reduction in viral load by week 4 of treatment (−3.2 vs −0.8 log IU/ml; p<2.2E-16). The rs12979860 CC genotype was also associated with wild type core70 (78% vs 54%; p=1.6E-6) and non-wild type ISDR (67% vs 83%; p=0.007).

The frequency of the rs8099917 risk allele (G) was 0.15 among all patients, 0.08 in SVR patients, 0.13 in TR patients and 0.26 in NVR patients. Patients with the rs8099917 TT genotype were significantly more likely to achieve an SVR than patients with GT or GG genotypes (53% vs 24%, OR=3.43, p=2.18E-12), and GT/GG patients were significantly more likely to show an NVR

Table 1 Patient profiles by response to treatment

	All (813)	SVR (366)	TR (176)	NVR (271)
Sex (M/F)	459/354	231/135	84/92	144/127
Age	58 (51–65)	56 (47–63)	60.5 (56–65.25)	59 (52.5–66)
Body weight (kg)	59 (52–67)	60 (52–68.25)	58 (51–66)	60 (52–66.4)
BMI (kg/m^2)	22.61 (20.81–24.65)	22.44 (20.46–24.58)	22.85 (20.85–24.89)	22.76 (21.12–24.63)
Hypertension (yes/no)	141/672	61/305	29/147	51/220
Diabetes (yes/no)	97/716	31/335	25/151	41/230
Fibrosis (0–2/3–4)	138/421	52/227	34/81	52/113
Activity (0–1/2–3)	274/272	136/138	53/56	85/78
ISDR (0, 1/≥2)	78/298	43/128	15/71	20/99
Amino acid 70 (wild-type/mutant)	256/139	137/45	54/35	65/59
Amino acid 91 (wild-type/mutant)	221/178	112/72	51/40	58/66
WBC (/L)	4.71×10^9 (3.9×10^9–5.7×10^9)	4.9×10^9 (4.0×10^9–6.0×10^9)	4.6×10^9 (3.8×10^9–5.4×10^9)	4.6×10^9 (3.7×10^9–5.5×10^9)
Haemoglobin (g/dl)	14.1 (13.2–15)	14.2 (13.3–15.22)	13.9 (13.1–14.8)	14.1 (13.05–14.9)
Platelets ($\times10^4$L)	16.1×10^6 (12.5×10^6–19.9×10^6)	17.1×10^6 (13.7×10^6–20.7×10^6)	15.5×10^6 (11.3×10^6–18.8×10^6)	15.1×10^6 (12×10^6–19.2×10^6)
AST (IU/l)	45 (34–65.5)	43 (32.25–64)	43.5 (33.25–66)	48 (37–66.5)
ALT (IU/l)	55 (37–87)	57 (37–92)	50 (33–78)	53 (39–82.5)
γGTP (IU/l)	40 (25–72)	36 (23–65.75)	36 (23–69)	52 (32–86)a
Albumin (g/dl)	3.9 (3.7–4.1)	3.9 (3.7–4.1)	3.8 (3.7–4)	3.8 (3.7–4.1)
Total cholesterol (mg/dl)	171 (150–192)	169 (149.2–192)	175 (158–191)	170 (148.5–192.5)
Viral load (log IU/ml)	6.5 (6.1–6.9)	6.4 (5.9–6.825)	6.6 (6.3–7)	6.6 (6.2–7)
PEG-IFN-α2b (μg)	80 (80–100)	80 (80–100)	80 (75–100)	80 (60–100)
PEG-IFN-α2b/kg (μg/kg)	1.19 (1.19–1.48)	1.36 (1.19–1.48)	1.19 (1.19–1.48)	1.19 (1.02–1.48)
Ribavirin (mg)	600 (600–800)	600 (600–800)	600 (600–800)	600 (400–800)
Ribavirin/kg (mg/kg)	8.9 (8.9–11.87)	10.29 (8.9–11.87)	8.9 (8.9–11.87)	8.9 (7.8–11.86)
rs12979860 (CC/CT/TT)	582/203/27	311/51/4	128/43/4	143/109/19
rs8099917 (TT/TG/GG)	588/199/25	311/51/3	132/40/4	145/108/18

For categorical data, the number of patients in each category is shown. For continuous data, the median and range are displayed.
ALT, alanine aminotransferase; AST, aspartate aminotransferase; BMI, body mass index; F, female; γGTP, γ-glutamyltranspeptidase; ISDR, interferon sensitivity-determining region; M, male; NVR, non-virological response; PEG-IFN, pegylated interferon; SVR, sustained virological response; TR, transient response; WBC, white blood cells.

(56% vs 25%; OR=0.26; p=3.33E-16). Patients with the rs8099917 TT genotype had marginally higher baseline viral load (6.6 vs 6.4 log IU/ml; p=0.077) but showed a significantly greater drop in viral load by week 4 of treatment (−3.1 vs −0.8 log IU/ml; p<2.2E-16). The rs8099917 TT genotype was also associated with wild-type core70 (79% vs 56%; p= 3.1E-6) and non-wild-type ISDR (68% vs 83%; p=0.015).

Viral substitutions

Patients who achieved an SVR had significantly lower initial HCV RNA levels than those who did not (6.4 vs 6.6 log IU/ml; p=2.1E-6). The 140 patients (17%) with a substitution at position 70 of the HCV core protein (core70) were significantly less likely to achieve an SVR than patients with wild type core70 (33% vs 53%; p=0.00019) and were significantly more likely to show an NVR (42% vs 25%; p=0.0013). The 179 (22%) of patients with a substitution at position 91 (core91) were marginally less likely to achieve an SVR (41% vs 50%; p=0.08) but were significantly more likely to show an NVR (37% vs 27%; p=0.039). The 78 (10%) of patients who had two or more substitutions in the ISDR of NS5A were only marginally less likely to achieve an SVR than those with wild-type ISDR (43% vs 55%; p=0.066) and were not more likely to show an NVR (33% vs 26%; p=0.24).

Predictive factors for an SVR

Significant univariate predictors for an SVR included patient clinical factors (age, sex, diabetes, platelet count, white blood cell count, haemoglobin level, γGTP level); SNP genotype (rs12979860 and rs8099917); and viral factors (baseline viral load and core70, core91 and ISDR substitutions) (table 2). Following multivariate analysis, only age, rs12979860 genotype, core70 substitution and baseline viral load were significant independent predictors (figure 1A). The joint effects of rs12979860 and core70 on response to treatments are illustrated in figure 2.

Predictive factors for an NVR

Significant univariate predictors for an NVR included age, rs12979860 and rs8099917 genotypes, core70 and core91 substitutions, diabetes, aspartate aminotransferase (AST), baseline viral load, platelet count, white blood cell count and γGTP levels (table 3). Following multivariate analysis only age and rs12979860 genotype remained as independent predictors (figure 1B).

Predictive factors for change in viral load by week 4 of treatment

Factors influencing virological response were assessed by examining change in viral load between the start of treatment and week 4. Using linear regression, sex, rs12979860, rs8099917, core70, core91, ISDR, baseline viral load, alanine aminotransferase (ALT), platelet count, white blood cell count, haemoglobin level and γGTP were found to be significant univariate predictors of change in viral load by week 4 (table 4). Independent factors included rs12979860, core70, ISDR, ALT, platelet count and γGTP. We also found a significant positive linear relationship between the total number of ISDR substitutions and change in viral load between week 0 and week 4 (slope=0.2; p=0.0047).

In patients with the favourable rs12979860 CC genotype, core70 wild type was a significant predictor of viral decline (p=0.007; figures 3A,B), but in patients with the CT or TT genotypes, viral decline did not vary with respect to core70 substitutions (p=0.18; figures 3C,D). Conversely, ISDR was not

Table 2 Predictors for a sustained virological response

	Simple			Multiple			
Variable	n	OR	p Value	n	OR	95% CI	p Value
Age	813	0.58	1.22E-08***	362	0.432	0.31 to 0.60	6.61E-07***
Sex (male vs female)	813	1.28	0.0006***	362	1.2	0.95 to 1.54	0.133
BMI (kg/m^2)	800	0.87	0.1286				
rs12979860 (CC vs TC/TT)	812	3.65	2.67E-14***	362	4.98	2.81 to 8.82	4.00E-08***
rs8099917 (TT vs GT/GG)	812	3.53	1.77E-13***				
Hypertension	813	0.92	0.6452				
Diabetes	813	0.53	0.005907**				
Core amino acid 70 (wild type vs mutant)	395	0.42	5.82E-05***	362	0.527	0.31 to 0.89	0.01575*
Core amino acid 91 (wild type vs mutant)	399	0.66	0.0419*				
ISDR	376	1.12	0.1627				
Viral load (log IU/ml)	695	0.68	2.09E-06***	362	0.77	0.62 to 0.96	0.02249*
Fibrosis (F0–1 vs F2–4)	559	0.74	0.0817				
Activity (A0–1 vs A2–4)	546	0.96	0.7975				
Total cholesterol (mg/dl)	663	0.86	0.2151				
AST (IU/l)	687	1.03	0.1069				
ALT (IU/l)	692	1.26	0.0920				
Platelets (×10^4/L)	694	1.49	3.57E-05***	362	1.39	0.97 to 1.99	0.073
WBC (/L)	693	1.31	0.0014**				
Haemoglobin (g/dl)	693	1.28	0.0043**				
γGTP (IU/l)	646	0.96	0.0052**				

Results of simple and multiple regression are shown. Factors with a p value <0.05 were included in the multivariate model. Variables were selected using stepwise selection. Asterisks indicate level of statistical significance: *<0.05; **<0.01; ***<0.001.
ALT, alanine aminotransferase; AST, aspartate aminotransferase; BMI, body mass index; γGTP, γ-glutamyltranspeptidase; ISDR, interferon sensitivity-determining region; WBC, white blood cells.

a significant predictor of viral decline in patients with the rs12979860 CC genotype (p=0.078; figures 4A,B), but patients with the CT or TT genotypes and two or more substitutions in the ISDR showed significantly greater viral decline by week 4 than patients with zero or one ISDR substitution (p=0.007; figures 4C,D).

DISCUSSION

In this study we showed that host factors (younger age, male sex, favourable IL28B SNP genotypes) as well as viral factors (baseline viral load, wild-type core70 and two or more substitutions in the ISDR) contribute to the successful outcome of PEG-RBV combination therapy. Although some of these factors independently predict an SVR or NVR in multivariate analysis, collectively they reflect a complex genotype-by-environment interaction involving common polymorphisms in both the virus and the human host.

Genetic variation within the human IL28 locus has been reported as the strongest pretreatment predictor of an SVR,[15] and the results of this study support this finding. Several tightly linked SNPs in the non-coding region of *IL28A* and *IL28B* have been shown to be associated with spontaneous viral clearance, rapid and early virological response and/or SVR following treatment with interferon and ribavirin for HCV genotype 1b.[9–15] *IL28A*, *IL28B* and *IL29* code for type III (λ) interferons, which are similar to type I interferons but use a different receptor and show high tissue specificity.[27 28] It has not been determined which, if any, of the reported SNPs directly affects function, but the functional SNP probably affects gene expression. IRF3- and IRF7-binding sites near the transcription start

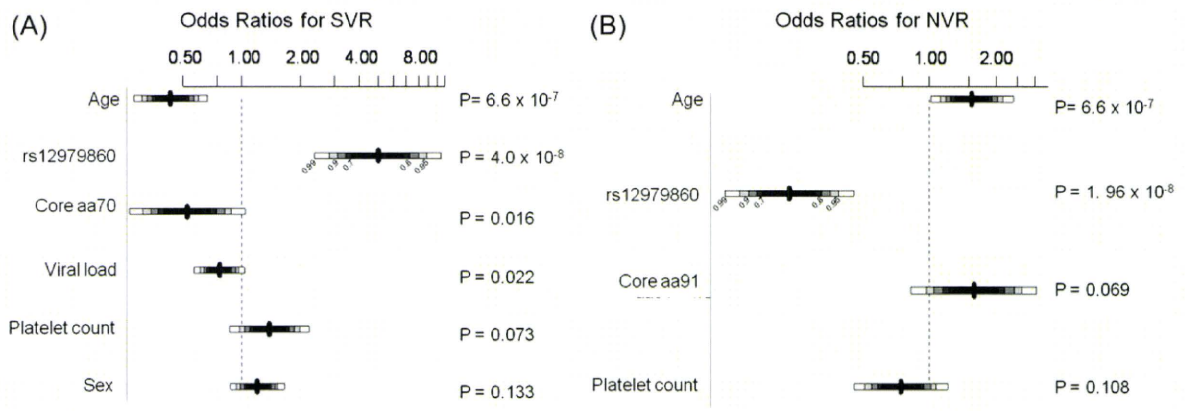

Figure 1 ORs for predictive factors response to treatment. ORs and 95% CIs are shown for predictive factors for (A) sustained virological response (SVR) and (B) non-virological response (NVR) based on multiple logistic regression with stepwise selection.

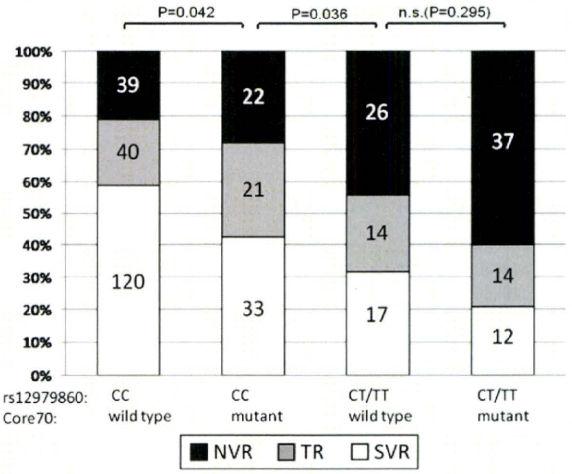

Figure 2 Cumulative effects of rs12979860 genotype and core protein amino acid 70 substitutions. The relative effects of rs12979860 genotype (favourable CC vs non-favourable CT/CC) and core amino acid 70 substitutions (favourable wild type vs unfavourable substitutions) on response to treatment are shown. NVR, non-virological response; TR, transient response/relapser; SVR, sustained virological response.

site of *IL28B* are essential for gene expression, but distal clusters of nuclear factor-κB (NF-κB)-binding sites are necessary for maximal expression,[29 30] suggesting that upstream polymorphisms may potentially disrupt transcription factor-binding sites within a distal promoter or enhancer. Unintuitively, interferon-stimulated genes are downregulated in patients with the favourable rs8099917 TT genotype,[31] implying that responders have a lower baseline expression of immune response genes.[32] This might serve to prevent desensitisation and promote maximal induction of interferon-stimulated genes, but detailed gene regulation studies are needed to resolve the role of IL28B polymorphisms in antiviral defence.

In addition to effects of human genetic polymorphisms, a number of studies have reported significant association between HCV core70/core91 substitutions and treatment outcome.[20 33 34] We found significant independent associations between core70 substitutions and an SVR, as well as change in viral load by week 4, but the association was not significant for an NVR under multivariate analysis despite being highly significant in univariate analysis. Although the role of core70 substitutions is unclear, the core protein interacts with a number of viral and host proteins and disrupts the interferon signalling pathway.[35–37] The proportion of core70 substitutions in the host viral population has been reported to increase during treatment with PEG-RBV therapy, which may indicate positive selection at this position in response to treatment.[38] Substitutions at these positions appear to affect the antiviral response during the early stages of treatment, as wild-type core70 and core91 are associated with a rapid decrease in HCV RNA levels during the first 4 weeks of treatment.[39 40] Because a rapid virological response is also a strong predictor of SVR and NVR, core70 and core91 substitutions may affect treatment outcome either directly or indirectly.[40 41]

Unlike HCV core70 substitutions, we found only a marginal association between ISDR substitutions and SVR, and no association with NVR. However, ISDR substitution was a significant independent predictor of change in viral load by week 4. The presence of two or more mutations in this 40 amino acid stretch of the NS5A protein is associated with an SVR.[24 42] Other studies have found no significant association between ISDR and SVR but have found a higher overall mutation rate in the NS5A protein among SVR patients,[43 44] and one study suggests that the association with ISDR varies by strain and is more pronounced in Japan than in Europe.[45] It is not clear whether mutations in ISDR directly affect function or whether they reflect the genetic distance from an interferon-resistant

Table 3 Predictors for a non-virological response

	Simple			Multiple			
Variable	**n**	**OR**	**p Value**	**n**	**OR**	**95% CI**	**p Value**
Age	813	1.30	0.01306*	370	1.55	1.12 to 2.15	0.008367**
Sex (male vs female)	813	0.90	0.178				
BMI (kg/m^2)	800	1.07	0.3899				
rs12979860 (CC vs TC/TT)	812	0.26	2.73E-17***	370	0.231	0.14 to 0.39	1.96E-08***
rs8099917 (TT vs GT/GG)	812	0.26	1.51E-17***				
Hypertension	813	1.16	0.4323				
Diabetes	813	1.55	0.04685*				
Core amino acid 70 (wild type vs mutant)	395	2.17	0.000496***				
Core amino acid 91 (wild type vs mutant)	399	1.66	0.02029*	370	1.58	0.96 to 2.60	0.06943
ISDR	376	0.92	0.06197				
Viral load (log IU/ml)	695	1.32	0.01716*				
Fibrosis (F0–1 vs F2–4)	559	1.24	0.2608				
Activity (A0–1 vs A2–4)	546	1.12	0.5499				
Total cholesterol (mg/dl)	663	0.98	0.5824				
AST (IU/l)	687	1.02	0.03148*				
ALT (IU/l)	692	0.91	0.8772				
Platelets (×10^4/L)	694	0.76	0.008222**	370	0.739	0.51 to 1.07	0.1077
WBC (/L)	693	0.83	0.04617*				
Haemoglobin (g/dl)	693	0.84	0.1201				
γGTP (IU/l)	646	1.15	1.23E-05***				

Results of simple and multiple regression are shown. Factors with a p value <0.05 were included in the multivariate model. Variables were selected using stepwise selection. Asterisks indicate level of statistical significance: *<0.05; **<0.01; ***<0.001.
ALT, alanine aminotransferase; AST, aspartate aminotransferase; BMI, body mass index; γGTP, γ-glutamyltranspeptidase; ISDR, interferon sensitivity-determining region; WBC, white blood cells.

Table 4 Predictors for change in viral load by week 4 of treatment

	Simple			Multiple		
Variable	**n**	**Coefficient**	**p Value**	**n**	**Coefficient**	**p Value**
Age	500	−0.01	0.138			
Sex (male vs female)	500	−0.23	0.005**			
BMI (kg/m^2)	494	0.00	0.958			
rs12979860 (CC vs TC/TT)	500	2.11	5.18E-38***	221	1.37	1.35E-08***
rs8099917 (TT vs GT/GG)	499	2.10	1.40E-36***			
Hypertension	500	−0.25	0.249			
Diabetes	500	−0.31	0.19			
Core amino acid 70 (wild type vs mutant)	259	−1.01	1.38E-05***	221	−0.665	0.001328**
Core amino acid 91 (wild type vs mutant)	262	−0.77	0.000***			
ISDR	247	0.20	0.006**	221	0.186	0.001878**
Viral load (log IU/ml)	500	0.37	0.000***	221	0.414	0.00012***
Fibrosis (F0–1 vs F2–4)	397	−0.22	0.217			
Activity (A0–1 vs A2–4)	389	−0.10	0.578			
Total cholesterol (mg/dl)	472	0.00	0.064			
AST (IU/l)	490	0.00	0.442			
ALT (IU/l)	493	0.00	0.005**	221	0.00606	0.008895**
Platelets (×10^4/L)	495	0.03	0.048*	221	0.0701	7.24E-05***
WBC (/L)	495	0.00	0.027*			
Haemoglobin (g/dl)	495	0.13	0.013*			
γGTP (IU/l)	460	0.00	0.001***	221	−0.00634	0.002095**

Results of simple and multiple regression are shown. Factors with a p value <0.05 were included in the multivariate model. Variables were selected using stepwise selection. Asterisks indicate level of statistical significance: *<0.05; **<0.01; ***<0.001.
ALT, alanine aminotransferase; AST, aspartate aminotransferase; BMI, body mass index; γGTP, γ-glutamyltranspeptidase; ISDR, interferon sensitivity-determining region; WBC, white blood cells.

strain. Nonetheless, the NS5A protein has been shown to be under purifying selection[44] and plays a critical role in both viral replication[46 47] and modulation of the immune response.[48] Therefore, the number of substitutions in one or more variable regions of the NS5A may be a useful predictor of early viral dynamics and an indirect predictor of SVR, although in this study we found a significant effect only for change in viral load by week 4 of treatment.

A number of factors have now been reported to influence outcome of PEG-RBV therapy, and it is important to determine which of these factors represent independent, clinically useful predictors. Because of the expense and occasionally severe side effects of the current standard of care, reliable pretreatment indicators, especially of poor response, will help guide treatment decisions and steer difficult-to-treat patients towards more

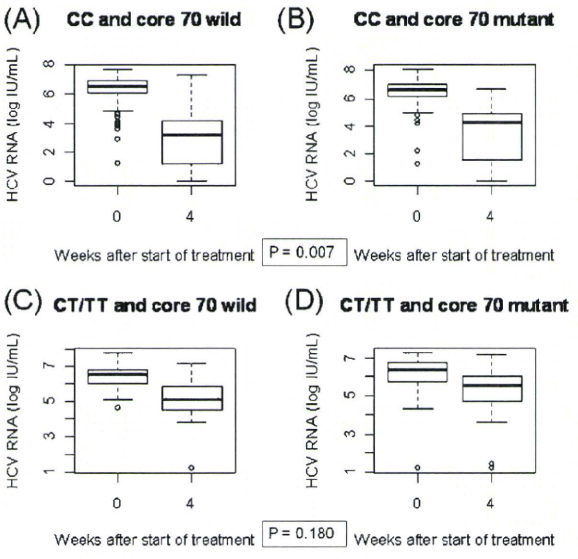

Figure 3 Change in viral load by IL28B single nucleotide polymorphism (SNP) genotype and hepapitis C virus (HCV) core protein substitutions. The change in viral load between the start of treatment and after 4 weeks plotted by rs12979860 genotype and wild/mutant amino acid at core70 is shown.

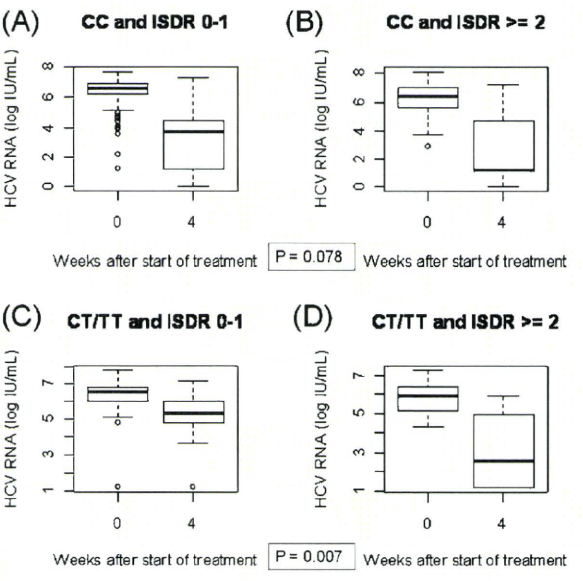

Figure 4 Change in viral load by IL28B single nucleotide polymorphism (SNP) genotype and substitutions in the interferon sensitivity-determining region (ISDR). The change in viral load between the start of treatment and after 4 weeks plotted by rs12979860 genotype and the number of substitutions in the ISDR is shown.

effective treatments or enrolment in clinical trials. In order to identify the most important independent predictors, it will be necessary to disentangle the intriguing interactions between human and viral polymorphisms as well as gain better understanding of the role of type III interferon in the immune response against HCV.

Acknowledgements We thank Mika Tsuzuno, Sakura Akamatsu, Sanae Furuya and other members of the clerical staff, and Yoshiiku Kawakami and other physicians at Hiroshima University Hospital for their help.

Funding This work was supported in part by Grants-in-Aid for scientific research and development from the Ministry of Health, Labor and Welfare, Government of Japan.

Competing interests None.

Ethics approval This study was conducted with the approval of the Hiroshima University ethics committee.

Provenance and peer review Not commissioned; externally peer reviewed.

REFERENCES

1. **Alter MJ.** Epidemiology of hepatitis C in the West. *Semin Liver Dis* 1995;**15**:5–14.
2. **Chevaliez S,** Pawlotsky JM. Hepatitis C virus: virology, diagnosis and management of antiviral therapy. *World J Gastroenterol* 2007;**13**:2461–6.
3. **Hadziyannis SJ,** Sette H Jr, Morgan TR, *et al.* Peginterferon-alpha2a and ribavirin combination therapy in chronic hepatitis C: a randomized study of treatment duration and ribavirin dose. *Ann Intern Med* 2004;**140**:346–55.
4. **Hijikata M,** Ohta Y, Mishiro S. Identification of a single nucleotide polymorphism in the MxA gene promoter (G/T at nt −88) correlated with the response of hepatitis C patients to interferon. *Intervirology* 2000;**43**:124–7.
5. **Knapp S,** Yee LJ, Frodsham AJ, *et al.* Polymorphisms in interferon-induced genes and the outcome of hepatitis C virus infection: roles of MxA, OAS-1 and PKR. *Genes Immun* 2003;**4**:411–19.
6. **Matsuyama N,** Mishiro S, Sugimoto M, *et al.* The dinucleotide microsatellite polymorphism of the IFNAR1 gene promoter correlates with responsiveness of hepatitis C patients to interferon. *Hepatol Res* 2003;**25**:221–5.
7. **Naito M,** Matsui A, Inao M, *et al.* SNPs in the promoter region of the osteopontin gene as a marker predicting the efficacy of interferon-based therapies in patients with chronic hepatitis C. *J Gastroenterol* 2005;**40**:381–8.
8. **Tsukada H,** Ochi H, Maekawa T, *et al.* A polymorphism in MAPKAPK3 affects response to interferon therapy for chronic hepatitis C. *Gastroenterology* 2009;**136**:1796–805, e6.
9. **Ge DL,** Fellay J, Thompson AJ, *et al.* Genetic variation in IL28B predicts hepatitis C treatment-induced viral clearance. *Nature* 2009;**461**:399–401.
10. **Tanaka Y,** Nishida N, Sugiyama M, *et al.* Genome-wide association of IL28B with response to pegylated interferon-alpha and ribavirin therapy for chronic hepatitis C. *Nat Genet* 2009;**41**:1105–9.
11. **Suppiah V,** Moldovan M, Ahlenstiel G, *et al.* IL28B is associated with response to chronic hepatitis C interferon-alpha and ribavirin therapy. *Nature Genetics* 2009;**41**:1100–4.
12. **Thomas DL,** Thio CL, Martin MP, *et al.* Genetic variation in IL28B and spontaneous clearance of hepatitis C virus. *Nature* 2009;**461**:798–801.
13. **Rauch A,** Kutalik Z, Descombes P, *et al.* Genetic variation in IL28B is associated with chronic hepatitis C and treatment failure: a genome-wide association study. *Gastroenterology* 2010;**138**:1338–45, e1–7.
14. **McCarthy JJ,** Li JH, Thompson A, *et al.* Replicated association between an IL28B gene variant and a sustained response to pegylated interferon and ribavirin. *Gastroenterology* 2010;**138**:2307–14.
15. **Thompson AJ,** Muir AJ, Sulkowski MS, *et al.* IL28B polymorphism improves viral kinetics and is the strongest pre-treatment predictor of SVR in HCV-1 patients. *Gastroenterology* 2010;**139**:120–9.
16. **Zeuzem S,** Franke A, Lee JH, *et al.* Phylogenetic analysis of hepatitis C virus isolates and their correlation to viremia, liver function tests, and histology. *Hepatology* 1996;**24**:1003–9.
17. **Kau A,** Vermehren J, Sarrazin C. Treatment predictors of a sustained virologic response in hepatitis B and C. *J Hepatol* 2008;**49**:634–51.
18. **Adinolfi LE,** Utili R, Andreana A, *et al.* Relationship between genotypes of hepatitis C virus and histopathological manifestations in chronic hepatitis C patients. *Eur J Gastroenterol Hepatol* 2000;**12**:299–304.
19. **Enomoto N,** Sakuma I, Asahina Y, *et al.* Comparison of full-length sequences of interferon-sensitive and resistant hepatitis-C virus 1b—sensitivity to interferon is conferred by amino-acid substitutions in the NS5A region. *J Clin Invest* 1995;**96**:224–30.
20. **Akuta N,** Suzuki F, Sezaki H, *et al.* Association of amino acid substitution pattern in core protein of hepatitis C virus genotype 1b high viral load and non-virological response to interferon—ribavirin combination therapy. *Intervirology* 2005;**48**:372–80.
21. **Desmet VJ,** Gerber M, Hoofnagle JH, *et al.* Classification of chronic hepatitis—diagnosis, grading and staging. *Hepatology* 1994;**19**:1513–20.
22. **Akuta N,** Suzuki F, Kawamura Y, *et al.* Predictive factors of early and sustained responses to peginterferon plus ribavirin combination therapy in Japanese patients infected with hepatitis C virus genotype 1b: amino acid substitutions in the core region and low-density lipoprotein cholesterol levels. *J Hepatol* 2007;**46**:403–10.
23. **Akuta N,** Suzuki F, Sezaki H, *et al.* Predictive factors of virological non-response to interferon—ribavirin combination therapy for patients infected with hepatitis C virus of genotype 1b and high viral load. *J Med Virol* 2006;**78**:83–90.
24. **Enomoto N,** Sakuma I, Asahina Y, *et al.* Mutations in the nonstructural protein 5A gene and response to interferon in patients with chronic hepatitis C virus 1b infection. *N Engl J Med* 1996;**334**:77–81.
25. **Ohnishi Y,** Tanaka T, Ozaki K, *et al.* A high-throughput SNP typing system for genome-wide association studies. *J Hum Genet* 2001;**46**:471–7.
26. **Suzuki A,** Yamada R, Chang X, *et al.* Functional haplotypes of PADI4, encoding citrullinating enzyme peptidylarginine deiminase 4, are associated with rheumatoid arthritis. *Nat Genet* 2003;**34**:395–402.
27. **Kotenko SV,** Gallagher G, Baurin VV, *et al.* IFN-lambdas mediate antiviral protection through a distinct class II cytokine receptor complex. *Nat Immunol* 2003;**4**:69–77.
28. **Marcello T,** Grakoui A, Barba-Spaeth G, *et al.* Interferons alpha and lambda inhibit hepatitis C virus replication with distinct signal transduction and gene regulation kinetics. *Gastroenterology* 2006;**131**:1887–98.
29. **Thomson SJ,** Goh FG, Banks H, *et al.* The role of transposable elements in the regulation of IFN-lambda1 gene expression. *Proc Natl Acad Sci USA* 2009;**106**:11564–9.
30. **Iversen MB,** Ank N, Melchjorsen J, *et al.* Expression of type III interferon (IFN) in the vaginal mucosa is mediated primarily by dendritic cells and displays stronger dependence on NF-kappaB than type I IFNs. *J Virol* 2010;**84**:4579–86.
31. **Honda M,** Sakai A, Yamashita T, *et al.* Hepatic ISG expression is associated with genetic variation in IL28B and the outcome of IFN therapy for chronic hepatitis C. *Gastroenterology* 2010;**139**:499–509.
32. **Li JH,** Lao XQ, Tillmann HL, *et al.* Interferon-lambda genotype and low serum low-density lipoprotein cholesterol levels in patients with chronic hepatitis C infection. *Hepatology* 2010;**51**:1904–11.
33. **Akuta N,** Suzuki F, Kawamura Y, *et al.* Predictors of viral kinetics to peginterferon plus ribavirin combination therapy in Japanese patients infected with hepatitis C virus genotype 1b. *J Med Virol* 2007;**79**:1686–95.
34. **Akuta N,** Suzuki F, Hirakawa M, *et al.* Association of amino acid substitution pattern in core protein of hepatitis C virus genotype 2a high viral load and virological response to interferon-ribavirin combination therapy. *Intervirology* 2009;**52**:301–9.
35. **de Chassey B,** Navratil V, Tafforeau L, *et al.* Hepatitis C virus infection protein network. *Mol Syst Biol* 2008;**4**:230.
36. **Ciccaglione AR,** Stellacci E, Marcantonio C, *et al.* Repression of interferon regulatory factor 1 by hepatitis C virus core protein results in inhibition of antiviral and immunomodulatory genes. *J Virol* 2007;**81**:202–14.
37. **Luquin E,** Larrea E, Civeira MP, *et al.* HCV structural proteins interfere with interferon-alpha Jak/STAT signalling pathway. *Antiviral Res* 2007;**76**:194–7.
38. **Kurbanov F,** Tanaka Y, Matsuura K, *et al.* Positive selection of core 70Q variant genotype 1b hepatitis C virus strains induced by pegylated interferon and ribavirin. *J Infect Dis* 2010;**201**:1663–71.
39. **Akuta N,** Suzuki F, Hirakawa M, *et al.* Amino acid substitutions in the hepatitis C virus core region of genotype 1b affect very early viral dynamics during treatment with telaprevir, peginterferon, and ribavirin. *J Med Virol* 2010;**82**:575–82.
40. **Hayashi K,** Katano Y, Ishigami M, *et al.* Mutations in the core and NS5A region of hepatitis C virus genotype 1b and correlation with response to pegylated-interferon-alpha 2b and ribavirin combination therapy. *J Viral Hepat* 2010; Epub ahead of print.
41. **Ishii K,** Shinohara M, Sawa M, *et al.* Interferon alpha receptor 2 expression by peripheral blood monocytes in patients with a high viral load of hepatitis C virus genotype 1 showing substitution of amino acid 70 in the core region. *Intervirology* 2010;**53**:105–10.
42. **Nakagawa M,** Sakamoto N, Ueyama M, *et al.* Mutations in the interferon sensitivity determining region and virological response to combination therapy with pegylated-interferon alpha 2b plus ribavirin in patients with chronic hepatitis C-1b infection. *J Gastroenterol* 2010;**45**:656–65.
43. **Jardim AC,** Yamasaki LH, de Queiroz AT, *et al.* Quasispecies of hepatitis C virus genotype 1 and treatment outcome with peginterferon and ribavirin. *Infect Genet Evol* 2009;**9**:689–98.
44. **Bittar C,** Jardim AC, Yamasaki LH, *et al.* Genetic diversity of NS5A protein from hepatitis C virus genotype 3a and its relationship to therapy response. *BMC Infect Dis* 2010;**10**:36.
45. **Pascu M,** Martus P, Hohne M, *et al.* Sustained virological response in hepatitis C virus type 1b infected patients is predicted by the number of mutations within the NS5A-ISDR: a meta-analysis focused on geographical differences. *Gut* 2004;**53**:1345–51.
46. **Masaki T,** Suzuki R, Murakami K, *et al.* Interaction of hepatitis C virus nonstructural protein 5A with core protein is critical for the production of infectious virus particles. *J Virol* 2008;**82**:7964–76.
47. **Gao M,** Nettles RE, Belema M, *et al.* Chemical genetics strategy identifies an HCV NS5A inhibitor with a potent clinical effect. *Nature* 2010;**465**:96–100.
48. **Pang PS,** Planet PJ, Glenn JS. The evolution of the major hepatitis C genotypes correlates with clinical response to interferon therapy. *PLoS One* 2009;**4**:e6579.

Journal of General Virology (2010), **91**, 1668–1677 DOI 10.1099/vir.0.019315-0

Practical evaluation of a mouse with chimeric human liver model for hepatitis C virus infection using an NS3-4A protease inhibitor

Naohiro Kamiya,[1] Eiji Iwao,[1] Nobuhiko Hiraga,[2,3] Masataka Tsuge,[2,3] Michio Imamura,[2,3] Shoichi Takahashi,[2,3] Shinji Miyoshi,[4] Chise Tateno,[3,5] Katsutoshi Yoshizato[3,5] and Kazuaki Chayama[2,3]

Correspondence
Kazuaki Chayama
chayama@hiroshima-u.ac.jp

[1]Pharmacology Department V, Mitsubishi Tanabe Pharma Corporation, Yokohama, Japan

[2]Department of Medicine and Molecular Science, Division of Frontier Medical Science, Programs for Biomedical Research, Graduate School of Biomedical Sciences, Hiroshima University, Hiroshima, Japan

[3]Liver Research Project Center, Hiroshima University, Hiroshima, Japan

[4]DMPK Department, Mitsubishi Tanabe Pharma Corporation, Kisarazu, Chiba, Japan

[5]PhoenixBio, Higashihiroshima, Japan

A small-animal model for hepatitis C virus (HCV) infection was developed using severe combined immunodeficiency (SCID) mice encoding homozygous urokinase-type plasminogen activator (uPA) transplanted with human hepatocytes. Currently, limited information is available concerning the HCV clearance rate in the SCID mouse model and the virion production rate in engrafted hepatocytes. In this study, several cohorts of $uPA^{+/+}/SCID^{+/+}$ mice with nearly half of their livers repopulated by human hepatocytes were infected with HCV genotype 1b and used to evaluate HCV dynamics by pharmacokinetic and pharmacodynamic analyses of a specific NS3-4A protease inhibitor (telaprevir). A dose-dependent reduction in serum HCV RNA was observed. At telaprevir exposure equivalent to that in clinical studies, rapid turnover of serum HCV was also observed in this mouse model and the estimated slopes of virus decline were 0.11–0.17 $\log_{10}$ h^{-1}. During the initial phase of treatment, the $\log_{10}$ reduction level of HCV RNA was dependent on the drug concentration, which was about fourfold higher in the liver than in plasma. HCV RNA levels in the liver relative to human endogenous gene expression were correlated with serum HCV RNA levels at the end of treatment for up to 10 days. A mathematical model analysis of viral kinetics suggested that 1 g of the chimeric human liver could produce at least 10^8 virions per day, and this may be comparable to HCV production in the human liver.

Received 17 December 2009
Accepted 17 February 2010

INTRODUCTION

Hepatitis C virus (HCV) is a major cause for concern worldwide. More than 3% of the world's population is chronically infected with HCV and 3–4 million people are newly infected each year (Wasley & Alter, 2000). Chronic HCV infection is relatively mild and progresses slowly; however, about 20% of chronic hepatitis C (CHC) carriers progress to serious end-stage liver disease (Lauer & Walker, 2001; Liang *et al.*, 2000; Poynard *et al.*, 2003). The current standard treatment for HCV infection is administration of pegylated alpha interferon (PEG-IFN) in combination with ribavirin (RBV) for 48 weeks. The overall cure rates with this intervention are 40–50% for patients with genotype 1 and more than 75% for patients with genotypes 2 and 3 (Fried *et al.*, 2002; Manns *et al.*, 2001). Several compounds that inhibit specific stages of the virus life cycle have been clinically evaluated (Manns *et al.*, 2007; Pereira & Jacobson, 2009). Telaprevir is a novel peptidomimetic slow- and tight-binding inhibitor of HCV NS3-4A protease, which was discovered using a structure-based drug design approach (Perni *et al.*, 2006). A rapid decline in viral RNA was observed in CHC patients treated with telaprevir (Reesink *et al.*, 2006) and an increased antiviral effect of a combination of telaprevir and PEG-IFN has been reported (Forestier *et al.*, 2007). Recent clinical trials of telaprevir in combination with PEG-IFN and RBV have indicated a promising material advance in therapy for CHC patients (Hézode *et al.*, 2009; McHutchison *et al.*, 2009). First-generation HCV-specific agents have been developed despite the lack of small-animal models for HCV infection. However, early emergence of resistant variants against novel antiviral agents is a concern. Thus, the use of two or more investigation agents is strongly recommended for

clinical studies in CHC patients (Sherman *et al.*, 2007). To ensure ethical and safe clinical trials, animal models continue to be necessary for the mechanistic evaluation of the ability of specific agents to inhibit the virus life cycle *in vivo* and to develop better therapeutic strategies, including combination regimens (Boonstra *et al.*, 2009). Several groups have developed a small-animal model for HCV infection using homozygous urokinase-type plasminogen activator (uPA)/severe combined immunodeficiency (SCID) ($uPA^{+/+}/SCID^{+/+}$) mice transplanted with human hepatocytes (Mercer *et al.*, 2001). These mice are susceptible to cell culture-grown HCV (HCVcc; Lindenbach *et al.*, 2006) and have been used to evaluate antiviral agents including IFN-α, BILN 2061 (an NS3-4A protease inhibitor) and HCV796 (an NS5B polymerase inhibitor) (Kneteman *et al.*, 2006, 2009; Vanwolleghem *et al.*, 2007). However, the HCV clearance rate in the SCID mouse model and the virion production rate in hepatocytes engrafted in the mouse liver are not fully understood. We also generated a mouse model with an almost humanized liver (Tateno *et al.*, 2004). Using this mouse model, we reported the infection of a genetically engineered hepatitis B virus (Tsuge *et al.*, 2005) and developed a reverse genetics system for HCV genotypes 1a, 1b and 2a after intrahepatic injection of *in vitro*-transcribed RNA as well as intravenous injection of HCVcc (Hiraga *et al.*, 2007; Kimura *et al.*, 2008). In this study, we demonstrated the rapid turnover of serum HCV RNA and the pharmacokinetics (PK) and pharmacodynamics (PD) of telaprevir treatment. We concluded after quantitative estimation and the use of a mathematical model that HCV production equivalent to that in the human liver is possible in engrafted hepatocytes in this mouse model.

RESULTS

Preliminary dose-finding study

At the beginning of this study, we attempted to determine an effective dose regimen for telaprevir in this mouse model. Nine mice were randomized and treated with telaprevir over three time periods (Table 1). The lifetime kinetics of serum HCV RNA and of human serum albumin (HSA) in blood are represented in Fig. 1. One mouse (A07) exhibited a rapid reduction in HSA in the blood, which indicated the instability of human hepatocyte grafts. As a rapid reduction in HSA levels was not observed in subsequent experiments, this mouse was excluded from the mean analysis. After 7 days of twice daily (BID) dosing in period 1, the mean $\log_{10}$ changes in HCV RNA from baseline ($\pm$SEM) after the 100 and 10 mg telaprevir kg^{-1} doses were -0.49 ± 0.094 and -0.53 ± 0.039, respectively, and no dose-dependent reduction was observed. During period 2, the dose frequency was changed from BID to three times daily (TID), and the time of serum sampling was also changed from 1 to 4 h after the last dose. After the 3-day treatment, the mean $\log_{10}$ changes of HCV RNA in 100 and 10 mg telaprevir kg^{-1} TID groups were -1.00 ± 0.166 and -0.28 ± 0.056, respectively, and the difference between the two groups was significant. To test the reproducibility of results, mice were treated with 10 or 100 mg telaprevir kg^{-1} TID for 10 days and then sacrificed 5 h after the administration of the last dose. The mean $\log_{10}$ changes in serum HCV RNA were -1.46 ± 0.265 and -0.27 ± 0.073 in the 100 and 10 mg kg^{-1} TID groups, respectively, and the difference between the means was significant.

Evaluation of HCV turnover in this mouse model

Because of the SCID nature of this mouse model, the virion clearance mechanism was of interest. Six mice with steady-state and high viral loads (9.7×10^5–1.2×10^8 copies ml^{-1}) were administered 200 mg telaprevir kg^{-1} TID for 4 days, with 5 h intervals between doses and a 14 h intermission from drug treatment each day. Because the $\log_{10}$ reduction in HCV RNA appeared to depend on the time of serum collection during the day (Fig. 2a), the mean $\log_{10}$ changes in HCV RNA were plotted against time and fitted to a linear regression model (Fig. 2b). The estimated slopes (i.e. $\log_{10}$ HCV reduction per hour) and 95% confidence intervals (CI) on days 1, 2 and 3 were -0.165 (-0.268 to 0.0616), -0.115 (-0.131 to 0.0990) and -0.153, respectively. These regression lines also suggested that extrapolated HCV loads at the actual times of the daily first doses were 0.0530, -0.220 and -0.0948 $\log_{10}$ copies ml^{-1}, respectively. Therefore, it appeared that the viral load

Table 1. Telaprevir dose-finding experiment

Period	Duration (days)	Frequency of dose (per day)	Dose (mg kg^{-1})	No. of mice	Mean $\log_{10}$ changes ± SEM	*P* value (*t* test)
1	7	2	100	4	-0.49 ± 0.094	0.7806
			10	3*	-0.53 ± 0.039	
			0	1	-0.47	
2	3	3	100	4*	-1.00 ± 0.166	0.0064
			10	4	-0.28 ± 0.056	
3	10	3	100	3	-1.46 ± 0.265	0.0125
			10	3	-0.27 ± 0.073	

*One mouse was excluded because of instability of human hepatocyte grafts.

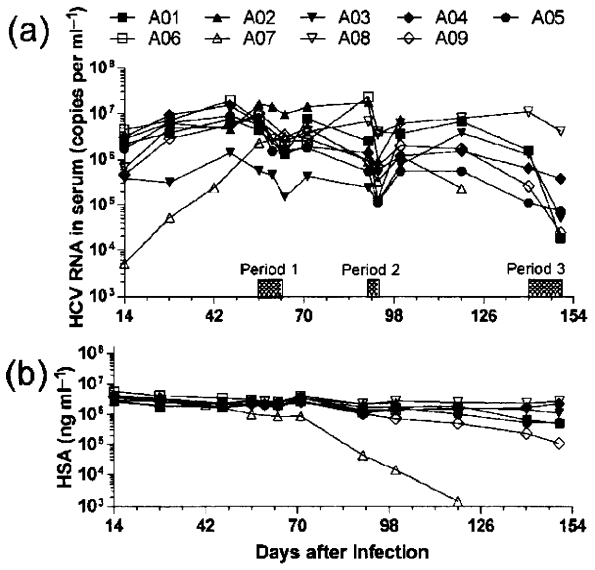

Fig. 1. Lifelong changes in serum HCV RNA and HSA in the blood of HCV-infected mice in the preliminary dose-finding experiment. Nine HCV-infected mice (A01–A09) were treated with telaprevir over three independent periods. The mice were treated with 10 mg telaprevir kg^{-1}, 100 mg telaprevir kg^{-1} or vehicle BID for 7 days (period 1), TID for 3 days (period 2) and TID for 10 days (period 3). (a) Kinetics of serum HCV RNA. (b) Kinetics of HSA level in blood. Because the HSA level indicated the stability of engrafted human hepatocytes in the mice, mouse A07 was excluded from the summary of the results in Table 1.

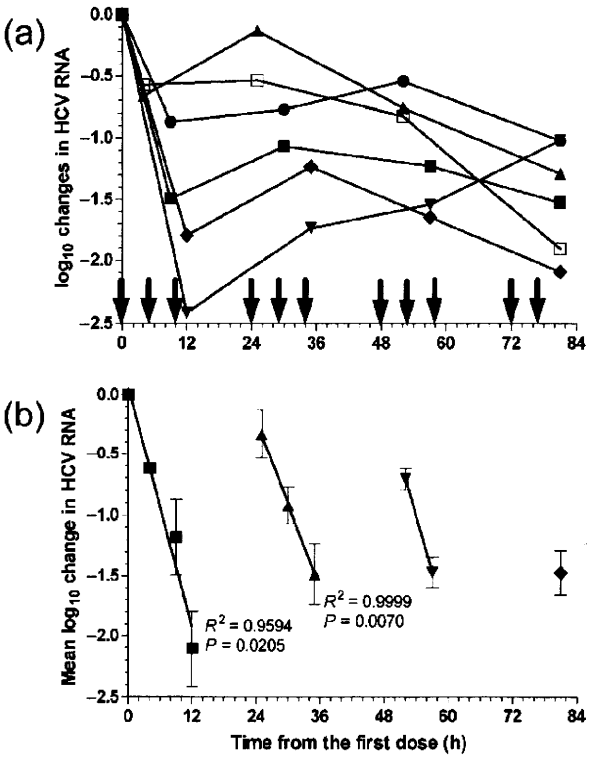

Fig. 2. Estimation of virus clearance rate. Six HCV-infected mice were treated with 200 mg telaprevir kg^{-1} TID for 4 days. Individual kinetics of $\log_{10}$ reductions in serum HCV RNA (a) and of mean $\log_{10}$ changes (±SEM) at each sampling time (b) are represented. Arrows indicate the times of dosing. The slopes of mean $\log_{10}$ HCV RNA reduction were estimated by linear regression analysis. P and R^2 values are indicated on the figure.

reverted back towards baseline levels during the 14 h intermission from drug treatment.

PK analysis

To assess drug exposure after repeated dosing in this mouse model, mice were administered 100 or 300 mg telaprevir kg^{-1} BID for 4 days. The mice receiving 300 mg kg^{-1} BID for 4 days had a mean 2 $\log_{10}$-fold HCV reduction, whereas those receiving 100 mg kg^{-1} BID had up to a 1.5 $\log_{10}$-fold reduction by day 3 (Fig. 3a). Plasma telaprevir concentrations after administration of the final dose are indicated in Fig. 3(b). The estimated half-life of telaprevir in the 100 and 300 mg kg^{-1} groups was 2.4 and 3.8 h, respectively.

PK/PD analysis and the dose-dependent reduction in HCV RNA

To evaluate the correlation between telaprevir concentration and HCV reductions in this mouse model, we used another cohort of 12 HCV-infected mice with high viral loads (1.6×10^6–3.9×10^8 copies ml^{-1}). In this crossover study, mice were randomized into three groups (n=4 each), each of which underwent two periods of dosing for 5 days separated by a 1-week washout period. Serum and plasma samples were collected once daily 5 h after dosing. The mean $\log_{10}$ changes in HCV RNA (±SEM) at different dose levels were calculated from the combined results of both periods (Fig. 4a). The mean $\log_{10}$ reductions from baseline in the 100 and 300 mg kg^{-1} groups were approximately 1 $\log_{10}$ and 1.5–2 $\log_{10}$, respectively, and the difference between the two groups was statistically significant. The means calculated in each period separately are also shown in Fig. 4(b). The plasma telaprevir concentration was positively correlated with the $\log_{10}$ HCV RNA reduction level in each period (Fig. 4c).

Drug concentrations and HCV levels in blood correlate with those in the liver

The correlation between telaprevir concentrations in the plasma and liver was analysed in a double logarithmic plot 5 (dose-finding cohort) or 8 h (PK and PK/PD cohorts) after the last dose (Fig. 5). The linear regression lines suggested that telaprevir concentrations in the liver were 5–

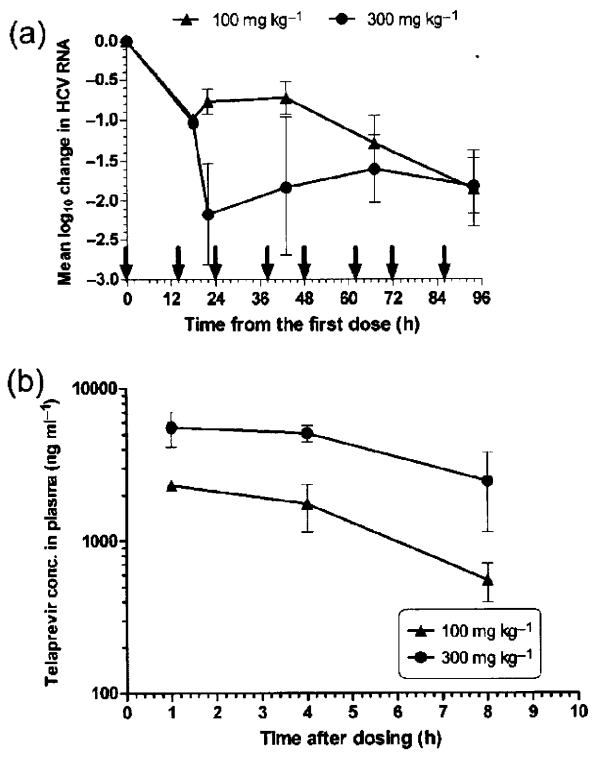

Fig. 3. PK analysis of telaprevir in the HCV-infected mouse model. Six HCV-infected mice were administered 100 (n=3) or 300 (n=3) mg telaprevir kg^{-1} BID for 4 days and serum samples were collected once daily to assess antiviral activity. After the last dose, plasma samples were collected at 1, 4 and 8 h for PK analysis. (a) Mean $\log_{10}$ changes (±SEM) in serum HCV RNA from mice treated with telaprevir. Arrows indicate the times of dosing. (b) Kinetics of telaprevir concentrations in plasma after the last dose.

10-fold higher at 5 h and approximately fourfold higher at 8 h than those in plasma. Total cellular RNA samples were extracted from two, one and four discrete small sections (approx. 50 mg) of the liver in the preliminary dose-finding, PK and PK/PD cohorts, respectively. HCV RNA levels in the total cellular RNA extract were relatively quantified by duplex real-time RT-PCR analysis using human β_2-microglobulin (hβ_2m) as an internal standard of human endogenous gene expression. Neither the threshold cycle (Ct) of hβ_2m ($Ct_{h\beta 2m}$) nor the Ct of HCV (Ct_{HCV}) correlated with total RNA from a small section of the chimeric human livers (data not shown). This result indicated that occupancy rates of human cells varied individually and/or among small sections of the chimeric human liver. Therefore, the mean difference in Ct ($\Delta Ct = Ct_{HCV} - Ct_{h\beta 2m}$) in each mouse was calculated and plotted against the viral load in serum (Fig. 6). After treatment with telaprevir for up to 10 days, mean ΔCt values ranged between 11 (HCV RNA content: $2^{11} = 2 \times 10^3$-fold lower than hβ_2m expression) and 17 (1×10^5-fold lower) among the HCV-infected mice and correlated linearly with $\log_{10}$ serum HCV RNA levels.

Viral dynamics model analysis

To evaluate time-dependent reductions in HCV with BID dosing, 12 HCV-infected elderly mice, which maintained high and steady-state viral loads (1.2×10^6–8.5×10^7 copies ml^{-1}) for more than 6 months, were treated with 200 mg telaprevir kg^{-1} BID for 3 days. The mice were divided into two groups, and serum samples were collected just before the second dose and 4 (n=6) or 8 (n=6) h after every two administrations. The single administration of telaprevir resulted in a mean 0.8–1.0 $\log_{10}$-fold reduction in HCV RNA in both groups. After the second dose, the pattern of viral kinetics appeared to depend on the time of serum collection, and the mean HCV RNA reduction level was higher in the 8 h group than in the 4 h group and plateaued at approximately a 2 $\log_{10}$-fold reduction in both groups after treatment for 3 days (Fig. 7). Finally, we attempted to estimate parameters of efficacy (ε) and virus clearance (c) per hour in this mouse model for comparison with estimates derived from human studies. Because the mean viral kinetics of the 8 h group was biphasic, the values in the 8 h group were used together for the mathematical model analysis. The estimated ε and c values were 0.992 (95 % CI 0.982–1.00) and 0.200 (95 % CI 0.110–0.291), respectively.

DISCUSSION

Using a mouse model with a chimeric human liver for HCV infection, we analysed the PK/PD of telaprevir treatment and investigated HCV dynamics during the initial phase of protease inhibitor treatment. All the mice in this study were expected to have more than half of their livers repopulated by human hepatocytes (Tateno *et al.*, 2004), which simulates a human drug metabolism profile (Katoh *et al.*, 2007, 2008). After the infection with HCV genotype 1b, high viral loads were maintained in the mice for more than 6 months. Recent studies have indicated the utility of a human/mouse chimera model for HCV infection to evaluate antiviral efficacy (Kneteman *et al.*, 2006, 2009) and preclinical safety (Vanwolleghem *et al.*, 2007). However, PK/PD studies and estimations of virus clearance rate have rarely been performed in this mouse model. HCV production, including intracellular replication in engrafted hepatocytes, has also not yet been elucidated. Despite the SCID nature of this mouse model, a 2 $\log_{10}$-fold HCV RNA reduction was observed within 0.5 days, as has been observed previously in CHC patients (Forestier *et al.*, 2007; Reesink *et al.*, 2006). In this mouse model, the rapid rebound in HCV load during the intermission from drug exposure indicated the rapid production and release of HCV into the circulation. This finding indicates that a virion-clearing compartment, which does not depend on T- and B-cell responses, may exist in this mouse model.

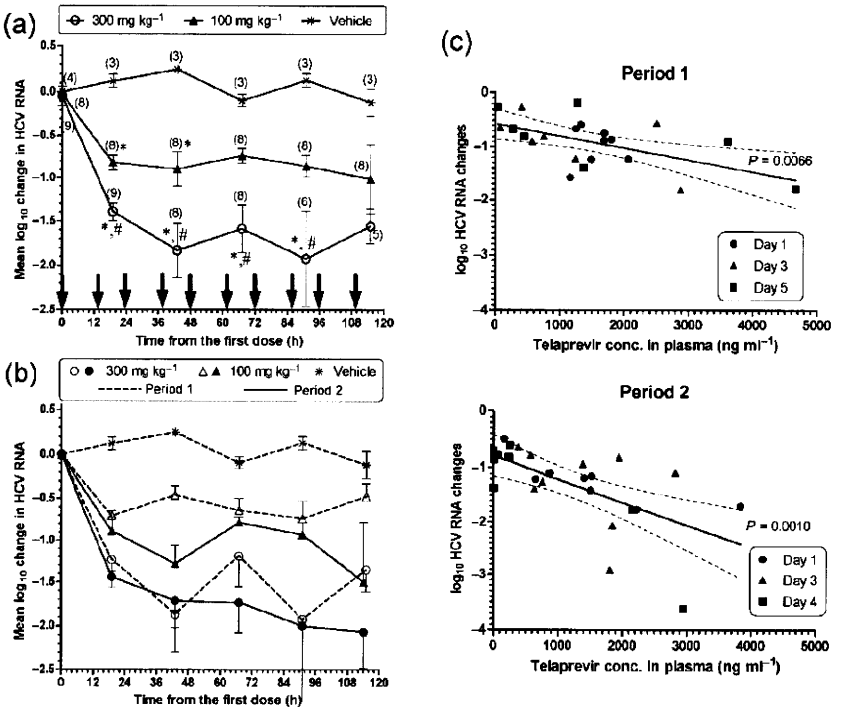

Fig. 4. PK/PD analysis and the dose-dependent reduction in HCV. Twelve HCV-infected mice were randomized into three groups (n=4 each) and then underwent two periods of telaprevir BID dosing for 5 days, separated by a 1-week washout period. Before the second period, the mice in the vehicle control group were additionally assigned to active drug groups. During the second period, mice that received the high or low doses were crossed over to the alternative treatment. Serum and plasma samples were collected once daily 5 h after dosing. Mean $\log_{10}$ changes (±SEM) in serum HCV RNA were calculated from the combined results from both periods (a) and each period separately (b). Arrows indicate the times of dosing. *, $P<0.05$ versus vehicle control group; #, $P<0.05$ versus 100 mg kg^{-1} group. (c) Correlation between $\log_{10}$ reduction in serum HCV and telaprevir concentrations in plasma. Linear regressions (solid lines) and 95% CI (dashed lines) are indicated.

One possible explanation is that viral kinetics after liver transplantation in humans may play a role in HCV clearance under immunosuppressed conditions (Dahari *et al.*, 2005; Powers *et al.*, 2006; Schiano *et al.*, 2005). This observation suggests that this mouse model is capable of evaluating 'first-phase' HCV clearance after drug treatment.

In a clinical trial of telaprevir, CHC patients who exhibited a continuous decline in viral kinetics had mean plasma trough levels above 1000 ng ml^{-1}; therefore, a dose of 750 mg TID was selected for further clinical studies (Sarrazin *et al.*, 2007). When HCV-infected mice were administered 100 or 300 mg telaprevir kg^{-1}, a plasma concentration above 1000 ng ml^{-1} was maintained beyond 8 h in mice treated with 300 mg kg^{-1} but not in those treated with 100 mg kg^{-1}. This result suggests that the extrapolation of telaprevir doses from this mouse model to human studies depends on body surface area, i.e. approximately 15th of a dose in this mouse model may be equivalent to a dose in humans. In another cohort of mice treated with 100 and 300 mg telaprevir kg^{-1} BID, a dose-dependent reduction in HCV was observed and the plasma telaprevir concentration correlated significantly with the HCV reduction level. Therefore, the PK/PD results in this mouse model may be able to indicate a targeted dose range in clinical studies.

Whereas a telaprevir concentration in plasma equivalent to its dosage in clinical trials was achieved in this mouse model, the serum HCV RNA level plateaued at a decrease of approximately 2 $\log_{10}$-fold within several days of treatment. A saturated reduction of approximately 2 $\log_{10}$-fold after treatments with BILN 2061 and IFN was also reported in an analogous mouse model (Kneteman *et al.*, 2006; Vanwolleghem *et al.*, 2007). These observations led us to examine HCV replication in the chimeric human liver. In the relative quantification of HCV RNA against human-specific endogenous gene expression, we observed a correlation between the serum HCV RNA level and the mean ΔCt value in the liver, despite no correlation between the total RNA concentration and each Ct value of two target genes in the liver RNA extracts. This result can be interpreted to indicate that HCV replicated only in

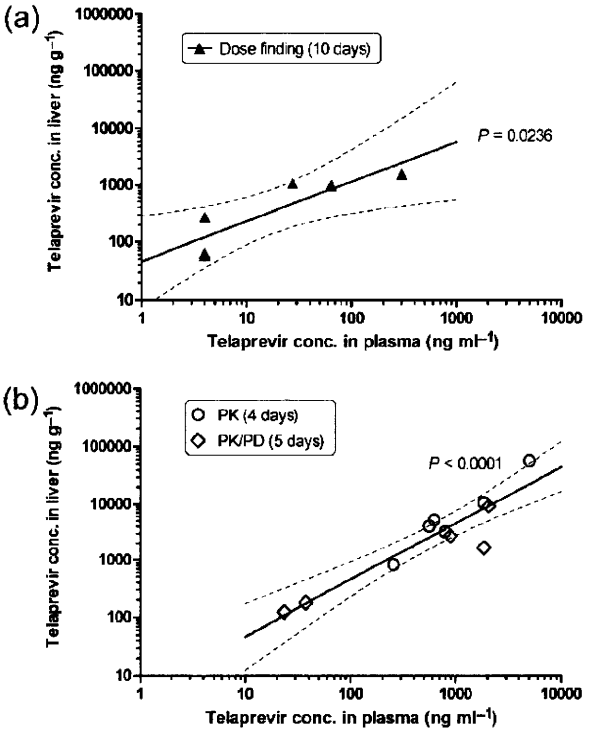

Fig. 5. Correlation between telaprevir concentrations in the liver and plasma. Telaprevir concentrations in the liver and plasma were determined at the end of the three different experiments indicated in Fig. 1 (dose-finding), Fig. 3 (PK) and Fig. 4 (PK/PD). Telaprevir concentrations in the liver were plotted against those in plasma 5 (a) or 8 (b) h after the last dose. Linear regressions (solid lines) and 95% CI (dashed lines) are indicated.

engrafted human hepatocytes, and the observed HCV reduction in serum might reflect virus replication in the human hepatocyte grafts. Moreover, the relative content of HCV RNA was 2×10^{3}–1×10^{5}-fold lower than hβ_2m expression, whereas an HCV replicon cell line, which had approximately 1000 replicon genomes per cell (Quinkert *et al.*, 2005), contained nearly equal amounts of both genes (data not shown). HCV replication was much lower in the engrafted human hepatocytes than in an HCV replicon cell line, and HCV infected only a small portion of the engrafted human hepatocytes. It has been reported that 4–25% of hepatocytes in a CHC patient were positive for replicative-intermediate RNA, and the mean number of viral genomes per productively infected hepatocyte ranged from 7 to 64 molecules (Chang *et al.*, 2003). Also, a more recent report suggested that the percentage of HCV antigen-positive hepatocytes in patients varied from 0 to 40%, and the HCV content in 2000 microdissected HCV-positive cells ranged from 40 to 1800 international units using a branched DNA assay (Vona *et al.*, 2004). Therefore, we suggest that HCV replication efficiency in engrafted human hepatocytes is equivalent to that in CHC patients.

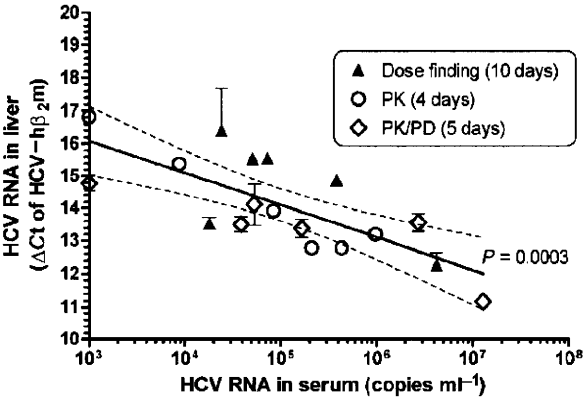

Fig. 6. Correlation between HCV content in the liver and serum. Relative quantification of HCV RNA levels in the liver was determined by the difference between threshold cycles (ΔCt) of HCV RNA and hβ_2m in a duplex real-time RT-PCR analysis. Linear regressions (solid line) and 95% CI (dashed lines) are indicated.

The differences observed between the engrafted human hepatocytes and the HCV replicon cell line can be explained by the following assumptions: approximately 10% of engrafted human hepatocytes are productively

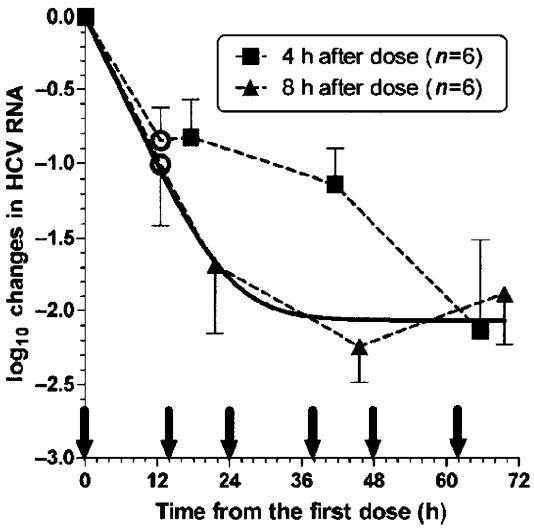

Fig. 7. Viral dynamics under BID telaprevir treatment. Mice were administered 200 mg telaprevir kg^{-1} BID at the times indicated by arrows. Serum samples were collected just before the second dose was administered and 4 (n=6) or 8 (n=6) h after every two doses were administered. Mean $\log_{10}$ changes (±SEM) in serum HCV RNA are plotted. The solved equation described in Methods was fitted to the values in the 8 h group (solid line), and the estimated efficacy and virion clearance rates were 0.992 (95% CI 0.982–1.00) and 0.200 (95% CI 0.110–0.291), respectively.

infected and harbour approximately ten HCV genomes per cell at baseline steady state and a 2 $\log_{10}$-fold reduction is achieved with drug treatment.

Mathematical models have proven valuable in understanding the *in vivo* dynamics of HCV, and very rapid dynamic processes occur on timescales of hours to days, and slower processes occur on timescales of weeks to months (Perelson & Ribeiro, 2008). In the last experiment, we observed a biphasic decline in the HCV RNA level after BID dosing for 3 days. During the first 2 days of the treatment, a discrepancy in viral kinetics between the serum-sampling time points was noted. Similarly, fluctuations in viral kinetics during the first-phase slope were observed in patients who received IFN three times a week (Pawlotsky *et al.*, 2004). Variable efficacy rate determined by PK parameters can explain fluctuations during the first-phase slope in mathematical model analysis (Talal *et al.*, 2006). However, it is difficult to evaluate the individual temporal changes in viral and drug kinetics using a mouse model as only a limited volume of blood is available for analysis. Therefore, we assumed a constant efficacy rate (ε) and omitted a turnover rate of hepatocytes because of the short duration of treatment. The estimated clearance rate (c) in this study was 4.8 day^{-1}. Additionally, the mean slope of 0.144 $\log_{10}$ h^{-1} (Fig. 2b) could be transformed to 0.332 h^{-1}=8.0 day^{-1} according to the change of base of a logarithm. The estimated clearance rates in this mouse model basically agreed with estimates determined in humans infected with HCV genotype 1 and undergoing IFN-based therapies (Herrmann *et al.*, 2003; Neumann *et al.*, 1998; Pawlotsky *et al.*, 2004) or large-volume plasma apheresis (Ramratnam *et al.*, 1999). Total virion production during steady-state viral kinetics in this mouse model was calculated by multiplying c by the initial viral load (V_0) and then normalizing the extracellular fluid volume. From previous studies, it was determined that 10^{11}–10^{13} virions are produced daily in patients with high HCV loads (Neumann *et al.*, 1998; Ramratnam *et al.*, 1999). In this mouse model, the volume of extracellular fluid and weight of the liver were approximately 20 and 9% of the body weight (data not shown), and the mean $\log_{10}$ V_0 ($\pm$SEM) among the mice with mean clearance rates of 4.8 and 8.0 per day were 6.96$\pm$0.26 and 7.00$\pm$0.33, respectively. The results of the calculations indicated that 1 g of the chimeric human liver produced 1×10^8–2×10^8 virions per day. The typical weight of the human liver is 1–2 kg; thus, the capacity of human hepatocytes to produce HCV in this mouse model may be equivalent to that in CHC patients. In conclusion, a mouse model with a chimeric human liver can simulate HCV replication in human patients quantitatively and dynamically, and this mouse model may be suitable for preclinical evaluations of novel HCV-specific agents and other therapeutic strategies, including combination regimens.

METHODS

Generation of mice with chimeric human livers and HCV infection. The generation of uPA$^{+/+}$/SCID$^{+/+}$ mice and transplantation of frozen human hepatocytes was performed at PhoenixBio. Graft function was monitored on the basis of HSA levels in blood (Tsuge *et al.*, 2005). All the mice had high HSA levels, which suggested that nearly half of their livers were repopulated by human hepatocytes (Tateno *et al.*, 2004). After obtaining written informed consent, we collected sera periodically from patients who were chronically infected with HCV genotype 1b and failed to respond to PEG-IFN and RBV therapy. The mice were inoculated with the serum samples via the orbital vein after anaesthetization. The experimental protocol was approved by the Ethics Review Committee for Animal Experimentation of the Graduate School of Biomedical Sciences, Hiroshima University.

Compound preparation and experimental designs. The telaprevir formulations were kindly provided by Vertex Pharmaceuticals. A telaprevir suspension was prepared as described previously (Perni *et al.*, 2006) and used in experiments 1 and 2. In the other experiments, a telaprevir suspension was prepared daily as in the tablet formulation (Forestier *et al.*, 2007; Hézode *et al.*, 2009; McHutchison *et al.*, 2009). A suspension of telaprevir was administered via oral gavage.

Experiment 1: preliminary dose-finding study. Ten out of 11 mice developed serum HCV loads greater than 10^4 copies ml^{-1}. Nine mice with high viral loads ($>10^5$ copies ml^{-1}) were randomized and administered 10 or 100 mg telaprevir kg^{-1} BID or TID over three periods. During period 1, the mice were administered 100 (n=4) or 10 (n=4) mg telaprevir kg^{-1} or vehicle (n=1) BID at 18:00 and 10:00 h for 7 days, and serum samples were collected before treatment and 1 h after administration in the morning on the third and/or seventh day. During period 2, the mice were administered 100 (n=5) or 10 (n=4) mg telaprevir kg^{-1} TID for 3 days, and serum samples were collected before treatment and 4 h after administration of the last dose. Three mice died between periods 2 and 3. During period 3, the mice were administered 100 (n=3) or 10 (n=3) mg telaprevir kg^{-1} TID for 10 days. The mice were sacrificed 5 h after administration of the last dose, and plasma, serum and liver samples were collected.

Experiment 2: evaluation of HCV turnover. Eleven mice were infected with HCV and eight mice survived for more than 15 weeks with steady-state and high viral loads (10^6–10^8 copies ml^{-1}). Six of the mice were administered 200 mg telaprevir kg^{-1} TID at 9:00, 14:00 and 19:00 h for 4 days. On day 1, serum samples were collected before dose administration, 4 h after the first and second doses were administered, and 2 h after the third dose was administered (n=2 each). On day 2, serum samples were collected 1 h after each of the three doses was administered (n=2 each). Serum samples were also collected 4 h after the first and second doses were administered on day 3 (n=3 each) and 4 h after the second dose was administered on day 4.

Experiment 3: PK analysis. After a washout period, six mice from experiment 2 were administered 100 or 300 mg telaprevir kg^{-1} (n=3 each) BID at 19:00 and 9:00 h for 4 days. Serum samples were collected before dose administration, 4 (n=1) or 8 (n=2) h after administration of the second dose, and 5 h after every two doses were administered. After the final dose was administered, plasma for PK analysis was collected at 1 and 4 h. The mice were sacrificed at 8 h, and serum, plasma and liver samples were collected.

Experiment 4: dose dependence and PK/PD analysis. Thirty-six mice were infected with HCV and 13 survived for more than 13 weeks. The median survival time of this cohort was 81 days after infection. Twelve HCV-infected mice were randomized into three groups (A–C; n=4 each) and underwent two periods of BID dosing for 5 days, which were separated by 1-week washout periods. During the first period, the mice in groups A, B and C were administered 300 mg telaprevir kg^{-1}, 100 mg telaprevir kg^{-1} and vehicle,